CHAPTER 8-- LANDSLIDE STABILITY ANALYSIS

In this chapter we analyze the impact of ski area development on slope stability on Snodgrass Mountain, by performing pre-development and post-development slope stability analyses, as recommended by Baum (1996) and RCE (1995). We performed static, limit-equilibrium slope stability analyses on 6 cross-sections on the SE flank of Snodgrass Mountain, using the geological, geophysical, and hydrological data described in Chapters 2-7. Those results are described in Section 8.2. But first, in Section 8.1 we consider how the presence or absence of historical landslides on Snodgrass Mountain and nearby slopes can provide a "reality check" on the computer stability simulations shown in Section 8.2.

8.1. Stability Analysis by Historic Analogy

The historic record of slope behavior on Snodgrass Mountain and nearby slopes forms a modern analog from which to predict future slope behavior. We have already described the historic landslides that have occurred on slopes similar to those of Snodgrass, including the Gold Link slide on Mt. Crested Butte (Chapter 2, Sec. 2.8).

Another way to assess the landslide hazard on Snodgrass Mountain is to examine its slope behavior during years of known precipitation and snowfall. According to the SNOTEL station on Mt. Crested Butte, the water years 1984 and 1995 were the snowiest in the past 24 years (Table 8-1).

Table 8-1. Snowpack water content, 1982-2005, from the Mt. Crested Butte SNOTEL site. Blue, more than 10% above normal; green, 0-10% above normal' yellow, 0-10% below normal; red, more than 10% below normal.

Year	% of Average Snowpack
1982	109%
1983	92%
1984	143%
1985	112%
1986	128%
1987	88%
1988	86%
1989	90%
1990	81%
1991	94%
1992	92%
1993	123%
1994	78%
1995	138%
1996	103%
1997	124%
1998	82%

Year (sorted by % of avg snowpack	% of Average Snowpack
1984	143%
1995	138%
1986	128%
1997	124%
1993	123%
1999	114%
1985	112%
1982	109%
2005	107%
1996	103%
1991	94%
2003	93%
1983	92%
1992	92%
1989	90%
2001	89%
1987	88%

1999	114%	1988	86%
2000	85%	2000	85%
2001	89%	1998	82%
2002	71%	1990	81%
2003	93%	2004	80%
2004	80%	1994	78%
2005	107%	2002	71%

According to all the publications we have reviewed, there were no reports of landsliding or landslide reactivation of Snodgrass Mountain in any of the years between 1982 and 2005. This includes the year 1984, which was described by Western Engineers (1986) based on their work at the base of Snodgrass. The implication is that snowpacks of 143% of average do not change slope stability conditions enough on Snodgrass to exceed the "threshold of stability" for reactivating large, thick landslides.

According to Resource Engineering (2008; Appendix 8-1 of this report), the predicted increase in water infiltration due to the proposed development actions, averaged over all of Snodgrass Mountain, is 10%. This is equivalent to the increased infiltration associated with a snowpack 110% of normal, based on the assumption that a constant 5% of any snowpack infiltrates into the subsurface. Thus, averaged over the entire Mountain, the predicted increase in infiltration due to the proposed development is similar to the increase that occurs between an average snowpack year (e.g., 1996) and a 110% average snowpack year (e.g., 1982).

Within individual sub-watersheds on Snodgrass, the predicted increase in infiltration due to development ranges from 0% (sub-watersheds in which there are no actions), to 68% (sub-watersheds with a very high proportion of trail clearing and snowmaking). However, only 5 of the 113 sub-watersheds (4%) have a predicted infiltration increase (due to development) of greater than 43% (A3-7, 68%; A7-4, 66%; E3-4, 61%; F2-4, 47%; A7-1, 44%). Recall that annual snowpack variations (and thus, infiltration) have been as high as +43% over the past 24 years, without triggering any observed landsliding on Snodgrass. Thus, this +43% value appears to be the "*minimum* threshold for slope instability" on Snodgrass. The predicted increase in infiltration due to proposed development is therefore less than the infiltration threshold for instability in 96% of the sub-watersheds. The implication is that proposed development in those 108 sub-watersheds will have a smaller impact to groundwater, than have the natural fluctuations in groundwater over the past 24 years. Because none of those natural fluctuations triggered landslide movement, we do not expect the proposed actions to trigger landslide movement in those 108 sub-watersheds, either.

For the 5 sub-watersheds where infiltration is predicted to increase more than 43%, we must ask if any landslides exist in those sub-watersheds. If not, then whatever the magnitude of groundwater fluctuations in the past hundreds or thousands of years, they would have been insufficient to cause landsliding.

However, all 5 watersheds contain some proportion of landslide deposits within them (Table 8-2).

Table 8-2. Reasons that 5 sub-watersheds have >43% increase in predicted infiltration to groundwater, in the post-development condition.

Sub-Watershed (WS)/ area (ac)	Predicted Increase in Infiltration	Reason for Increase	Proportion of Sub-Watershed underlain by Landslides	Need for Mitigation (for details, see Chapter 9)
A3-7/ 3.3 ac	68%	Trail 1 with snowmaking covers about half the WS	100% (mainly Qlsi, some Qefy)	Qlsi is probably not a problem; Qefy should be mitigated
A7-1/ 0.8 ac	44%	Trail 27 with snowmaking covers about 1/3 of WS	The eastern 50% (Qlsi)	Groundwater drains my be best here; convey water to axial drainage
A7-4/ 3.0 ac	66%	Trail 27 with snowmaking covers the NE half of the WS	About 1/6 of the WS is landslides; the rest is stable bedrock	Can be mitigated with same drain system as for WS A7-1
E3-4/ 14.0 ac	61%	Trail 30 with snowmaking covers about 55% of WS	Only the eastern 1/3 underlain by slides (Qlsiy, Qlsi, Qlso)	Easiest mitigation is shifting snowmaking to N, off of Qlsiy
F2-4/ 44.9 ac	47%	Trail 10 with snowmaking covers about 40% of WS	About 10% of WS underlain by slides, but includes Qlsh	Easiest mitigation is shifting snowmaking to N, off of Qlsh and Qlsy

Based on this reasoning by historic analogy, the landslides that lie partially in these 5 watersheds could possibly be destabilized by the proposed action. Thus, they should be mitigated until the Infiltration Ratio falls below 1.43, or if this cannot be done, they should be the subject of more detailed stability studies.

8.2 Analysis by Predictive Modeling-- METHODS

The standard method of quantitatively assessing landslide stability is performing a limit-equilibrium stability analysis of a 2-dimensional cross-section extending from the head to the toe of the landslide (Cornforth, 2006).

8.2.1 Construction of geologic cross-sections from boreholes and geophysics

The cross-sections used for stability analysis were constructed based on the geophysics lines, as follows. First, the interpreted S-wave tomograms of each spread on a given line were mosaicked together. We believe that S-wave velocities more truly depict material changes, unaffected by the complicating presence of groundwater. These mosaicked tomograms contained a line showing Zonge Geophysics' pick of the top of weathered Mancos Shale (details are given in Chapter 3).

Second, we superimposed the boring logs onto the tomograms. Third, based on the Zonge pick for top of bedrock and top of bedrock in the borings, we drew the inferred top of bedrock by roughly following the 7500 fps contour (see

Chapter 3). Fourth, we added additional deposit boundaries within the overlying Quaternary section, if borehole logs indicated such existed. These boundaries were extended away from the borehole along lines of relatively constant S-wave velocity. If the boundary was the bottom of a landslide deposit, we brought the boundary up to the ground surface at the toes of the headscarp and toescarp.

Well logs above the steep slope band generally show a 10-20 ft-thick weathered shale unit distinguishable from dry, in-situ Mancos Shale. Therefore, in the stability cross-sections we added a weathered shale unit in those parts of the section above the Pinedale glacial limit. Below the glacial limit, till or landslide deposits generally lie directly on unweathered shale. We thus assume that the thin zone of weathered shale was eroded by the passage of Pinedale glaciers. This same line of reasoning was applied to all stability cross-sections, with this result: above the glacial limit, failure planes with lowest Factor of Safety are generally predicted to occupy the zone of weathered shale that underlies relatively thin landslide deposits. In contrast, below the glacial limit failure planes with the lowest Factor of Safety are generally predicted to occupy the lowest parts of the over-thickened deposits of Pinedale till (Qpt) or old landslide deposits (Qlso).

8.2.2 Geotechnical Testing

Altogether we tested 13 samples for dry density, moisture content, angle of internal friction, and cohesion. These samples were taken from the vicinity of all three major cross-section lines (West, Central, East), and duplicated formations or deposit types in those areas (in case there were differences). The two strength parameters were measured in a direct shear apparatus for both peak and residual strengths. Details are given in Chapter 4.

8.2.3 Computer slope stability analysis

For landslides with any morphologic evidence for rotational movement, we used the Modified Bishop stability routine in the PCSTABL5M software package (Achilleos, 1988) and generated the weakest 10 trial failure surfaces. For very long landslides lacking such evidence (such as the young earthflow), we used the PLANAR subroutine.

8.2.4 Geotechnical Input Parameters

For landslide stability modeling, we used mainly test values from samples collected at Snodgrass (Table 8-3). However, we supplemented these values with values from Mt. Crested Butte and elsewhere in Colorado and Utah.

Table 8-3. Densities and shear strength parameters of geologic units from Snodgrass Mountain, derived by laboratory measurements on split-spoon samples and trench wall samples collected in July, 2007 (from Chapter 4).

Geologic Unit/ CROSS-SECTION/ sample*	Wet Unit Weight (pcf) **	Dry Unit Weight (pcf)	Peak		Residual	
			Friction (degrees)	Cohesion (psf)	Friction (degrees)	Cohesion (psf)
Qpt/ WEST/ 13-7	131	116.5	30.6	870	13.8	330
Qpt/ CENTRAL/ 14-7	118	107.7	45.5	170	-	-
Qot/ CENTRAL/ 14-9	135	121.7	46.3	0	19.2	140
Qefy/ CENTRAL/ 6-6	122	112.2	42	0	23.1	0
Qlsy/ EAST/ UT-10	110	101	25.3	560	18.7	170
Qlsio/ WEST/ 9-8	130	116.9	27.5	390	25.2	190
Shear zone/ EAST/ LT-1	121	106.2	40.3	150	22.5	0
Wx shale/ WEST/ 8-11	128	111.2	40	50	11.7	260
Wx shale/ CENTRAL/ 1-7	126	115	33.2	350	17.9	74
Km/ WEST/ 8-13	127	108.1	29.8	150	10.5	120
Km/ CENTRAL/ 4-15	96	93.4	39.5	0.0	10.5	0.0

* Qpt, Pinedale till; Qot, older till; Qefy, young earthflow; Qlsy, young landslide; Qlsio, intermediate-old landslide; shear zone, 10-40 cm-thick shear zones exposed in trenches; Wx shale, weathered shale; Km, Mancos Shale; samples list piezometer number followed by sample number (see Table 4-6).
**Samples were soaked a minimum of 24 hours each.

8.2.4.1 Landslide thickness

Landslide thickness was based on: (1) depth at which boreholes encountered in-place Mancos Shale, according to the geologist's well log, and (2) between drillholes, depth of the sudden increase in S-wave velocity in the seismic tomograms to greater than ~2500-3000 ft/sec.

8.2.4.2 Unit weight

Laboratory density values are shown in Table 8-3, and the preferred values used in the stability analyses are shown in Table 8-4.

Table 8-4. Density and shear strength input values for geologic units used in stability analyses on Snodgrass Mountain.

Geologic Unit	Wet Unit Weight (pcf)	Peak		Residual	
		Friction (degrees)	Cohesion (psf)	Friction (degrees)	Cohesion (psf)
Qpt (Pinedale till)	131	31	870	14	330
Qot (older till)	135	46	0	19	140
Qefy and Qefo (earthflow)	122	42	0	23**	0**
Qlsy and Qlsi (landslide deposits)	130	27	390	19 ***	170***
Shear zone	121	40	150	22	0
Weathered Mancos Shale	127	33	50	12	74
Unweathered Mancos Shale	127	30	150	10.5 17*	0 0
Tertiary porphyry		31	2000		

* for strongly-rotational landslides (slumps) ** for Qefb (polygon 1), use 25/0
*** for Qlsio and Qlso, use 25/190

8.2.4.3 Cohesion

The cohesion used in stability runs was the residual cohesion for each material, as indicated in Table 8-4.

8.2.4.4 Friction Angle

The friction angle used in stability runs was the residual friction for each material, as indicated in Table 8-4. These values are derived from the test data in Table 8-3, and represent either a rounded test value (for geologic units with only one test sample), or the lower test value (for geologic units with more than one test sample).

The strengths assigned to the unweathered Mancos Shale are handled differently than the others, for four reasons. First, several of the initial trial stability runs predicted failure when the laboratory residual strength values for Mancos Shale were combined with the summer 2007 groundwater conditions. Because no failure was occurring at that time (according to our personal observations, survey stake and inclinometer data), these lab strengths were clearly lower than the actual field strength of the entire failure plane. As a result, we altered lab strengths as explained below, to account for geologic and morphologic differences between landslides.

Second, if there is a zone of weathered shale atop unweathered shale (this occurs most places above the glacial limit), we assign residual strength to the weathered shale unit but peak strength to the unweathered shale unit. We do this because trial surfaces with low factors of safety tend to cluster either in the weathered shale zone, or immediately beneath it in the uppermost part of the unweathered shale. This clustering suggests that the weathered shale zone is the most likely locus for failure, rather than (say) a thin bed at residual strength within the unweathered shale.

Third, well logs suggest that the passage of Pinedale glaciers resulted in erosion of the pre-glacial zone of weathered shale. This results in Quaternary deposits lying directly on unweathered shale below the Pinedale glacial limit.

Fourth, where Quaternary deposits lie on unweathered shale, trial surfaces with low factors of tend to stay within the Quaternary deposits if they are thick, but penetrate into Mancos Shale is Quaternary deposits are thin. In the latter case, the Factor of Safety is very sensitive to what friction value is assigned to the unweathered Mancos Shale. Based on the drilling blow counts and the appearance of the drive samples, we assume that the unweathered shale has higher strength when forced to break across bedding, than along bedding.

Therefore, if the low-FS trial failures surfaces tend to be shallow arcs that could parallel the bedding direction in the shale (5-8° SE) over much of their length, we assign the laboratory residual strength to the shale (10.5°/ 0 psf). In contrast, where strongly-curved failure arcs are demanded by the landslide surface morphology and dimensions (such as polygons 9, 21, 22), only a small part of the arc can be following a bedding plane. In such cases we assign a higher residual strength to Mancos Shale in the computer model, to represent the fact that most of the failure plane has broken across (rather than along) bedding, and likely has more ruggedness and irregularity there than along a bedding plane

(such as the East Slide). The most common friction angle we use is the weighted average of the 2/3 the laboratory residual strength (to represent the throughgoing shear plane created by prior landsliding) and 1/3 the laboratory peak strength (to represent the higher ruggedness on the steeply-dipping parts of the failure plane). This weighted average friction angle is 17°. (Coincidentally, one of our 2 samples of weathered shale yielded a similar residual strength of 17.9°).

8.2.4.5 Saturated zones and pore pressures

After the geologic deposit boundaries were drawn on the cross-section based on S-wave velocities, we then constructed a matching mosaic of the P-wave tomograms. Next, we superimposed the borehole logs onto it. Noting where the water table lay in the boreholes, we drew the top of the inferred groundwater between the boreholes. This line defines the piezometric surface. Where the aquifers were unconfined (based on piezometer behavior), this line follows the P-wave velocity of approximately 5000 fps (saturated materials). Where aquifers are confined, this piezometric surface does not necessarily coincide with any particular P-wave velocity.

If the piezometric surface drawn in this way contained very steep or very flat gradients, or had a depression in it, we subjectively smoothed the curve a bit so that there were no depressions, or reaches of upslope flow (reversed gradient) or no flow (zero gradient). This is the way we defined the pre-development piezometric surface.

In order to estimate how much the piezometric surface rises due to the proposed action, Resource Engineering calculated the ratio of Infiltration in each sub-watershed (post-development:pre-development) (Appendix 8.1). This ratio was based on the trail/snowmaking map of 21-JUN-2007 developed by International Alpine Designs (Vail, CO), and is only valid for that design layout. Then, on each of the 6 slope stability cross-section lines we analyzed, we computed the weighted mean Infiltration Ratio along each cross-section, from the Infiltration Ratios of the sub-watersheds that the section crossed. For example, the Central Line, S Half cross-section is 1580 ft long and crosses parts of 5 sub-watersheds (subbasins), which have Infiltration Ratios ranging from 1.34 (moderate impact from development) to 1.0 (no impact from development). The length-weighted average of these ratios along the 1580 ft of cross-section is 1.12, representing a 12% increase in annual infiltration along the section.

Table 8-5. Example of method for estimating infiltration increases along a geologic cross-section due to development.

Cross-Section Name	Subbasin Crossed	Length of Subbasin Crossed		% of total line length	Subbasin Infiltration Ratio	Weighted Infiltration Ratio
		Begin (ft)	End (ft)			
	A3-5	0	280	0.18	1.34	0.24
	A3-4	280	380	0.06	1.16	0.07
	A2-6	380	600	0.14	1.08	0.15
	C1-5	600	1400	0.51	1.07	0.54
Central, S half	C1-6	1400	1580	0.11	1	0.11
		Weighted Infiltration Ratio of Entire Section				**1.12**

We then make the conservative assumption that all the increase in infiltration along the section goes to recharging groundwater in the landslides, rather than to (for example) shallow throughflow that reappears as streamflow on the mountain slopes (see the conceptual model described in Chapter 7, Sec. 7.2.3.1). This assumption is quite conservative, because the water balance model for the SE flank of Snodgrass indicates that about 50% of infiltration becomes discharge to on-mountain streams via shallow flowpaths (see Chapter 6, Sec. 6.4.3.3).

Finally, in order to transmit the increased subsurface flow resulting from development (e.g.,112% of pre-development flow, as on the Central Line, S Half; see Table 8-5), unconfined aquifers must be thickened by 12% to transmit the increased flow in the post-development condition. Because the bottom of the unconfined aquifer is essentially pinned at the top of shale bedrock, this thickening can only be accomplished by raising the water table by 12% of the aquifer thickness, all along the cross-section line.

Our baseline data for water table depths and piezometric surfaces comes from the period Nov. 2006 through Jan. 2008.

The stability analysis results (Factors of Safety) contain some degree of uncertainty, due to measurement error and intrinsic variability in the input data. This uncertainty could be assessed in two ways: (1) by running many permutations of each stability analysis with varying input data, drawn from the probability distribution function (PDF) of each input variable (Monte Carlo analysis, such as done by the USFS LISA software), or (2) using the most conservative input values (weakest strengths, greatest pore pressures, etc.) in a single stability analysis. In this study, we have insufficient test data to define PDFs for density, friction, and cohesion; nor can we generate PDFs for water table depth and landslide depth. Therefore, we followed the more-standard approach of using “conservative” input parameters. Below, we list whether our chosen input parameters are conservative (lead to lowest Factors of Safety), neutral, or non-conservative:

Density: used average value (**neutral**)

Friction: For shallow arcs and translational slides: used lowest value of residual friction angle after the method of Blake et al. (2002)(**triply conservative**, from Blake method, assumption that residual strength has been achieved throughout the deposit, AND that lowest angle value is representative of entire failure plane);
For strongly rotational slides (slumps), assigned an averaged peak/residual strength to Km (**neutral?**)

Cohesion: used lowest value of residual cohesion after the method of Blake et al. (2002)(**triply conservative**, from Blake method, assumption that residual strength has been achieved throughout the deposit, AND that lowest angle value is representative of entire failure plane);

For strongly rotational slides (slumps), assigned an averaged peak/residual strength to Km (**neutral?**)

Landslide thickness: used observed value (**neutral**)

Piezometric Surface: Pre-Development; used highest value (**conservative**) observed in piezometers during our period of record; our 22-month period of record (Nov. 2006-Jan. 2008) experienced slightly above average precipitation (107% of normal; **conservative**)

Post-Development; assumed that 100% of increased infiltration becomes added to groundwater flow in the landslides; this assumption may be **over-conservative** by 200%

In summary, the Factors of Safety cited hereafter are not mean values for the pre- and post-development conditions, as they would have been if the input values had "neutral" conservatism. Instead, the pre-development Factors of Safety cited are probably about mean minus 1 standard deviation. The post-development Factors of Safety are even more conservative (mean minus 2 standard deviations?), due to the assumption that 100% of infiltration adds to groundwater flow in the landslide.

8.3 Analysis by Predictive Modeling-- RESULTS

Due to the large number (57) of individual landslides mapped in this study, it was impractical to perform a separate stability analysis for each landslide. As a compromise, we clustered the drilling and geophysics along 3 long slope-stability transects on the SE flank of Snodgrass (West, Central, and East Sections). We then divided the Central Section into two sub-sections, above and below the steep slope band, and added separate analyses for critical young landslides such as the Ken's Crux slump (polygon 22) and the young earthflow (polygon 1). Altogether, we analyzed 6 stability cross-sections, and 1 to 2 individual landslides per section, as described below (Table 8-6).

8.3.1 West Cross-Section

The West cross-section is coincident with the West Line of the geophysical survey (Chapter 3), and crosses the West Slide Complex in a NW-SE direction and is about 2500 ft long (Fig. 8-1). The section begins at the base of the West Facet, traverses the West Slide Complex, and descends the steep slope band to end on the Old Earthflow at its base. Most of the section is underlain by intermediate (Qlsi) to old (Qlsio) landslides of the West Slide complex. As the section descends the steep slope band it transects a small younger landslide (Qlsiy, polygon 9), which probably represents failed glacial till deposited below the Pinedale glacial limit (about 9840 ft elevation). The slope below polygon 9 is still covered with till, and much of the old earthflow is likewise derived from Pinedale till.

The geologic contacts on the interpreted section (Fig. 8-2) were derived from the well logs of 3 piezometers (from south to north, PZ-13A/B, PZ-9. and PZ-8) and from the S-wave tomogram (Fig. 8-1). These sources indicate that

landslide deposits are roughly 40-60 ft thick atop Mancos Shale on the flatter parts of the West Slide complex. The uppermost 10-15 ft of shale beneath the West Slide Complex (e.g., PZ-8 and PZ-9) was logged as “weathered shale”, which was softer and moister than the underlying dry, hard, unweathered Mancos Shale.

Slide deposits thin to 20-40 ft thick on the steep slope band. The groundwater table was deduced from PZ-8 and -9, with minor adjustments to nearly follow the 5000 ft/sec contour on the P-wave tomogram.

Table 8-6. Summary table of Factors of Safety from landslide stability analyses. **Bold indicates the final, preferred analyses;** for a table showing all analyses, see Appendix 8-x. Post-development values are **shaded**..

CROSS-SECTION	POLYGON	GEOLOGY SECTION FILENAME/ DATE	WATER TABLE	ANALYSIS FILENAME/ PAGE	FACTOR OF SAFETY	REMARKS
WEST	9	Mirror mosaic of S lines v4.pdf/ 2/3/2008	Pre-Development	20080324141634796.pdf PAGE 1	1.37	Km 17°/0
WEST	9		Post-Development	20080324141634796.pdf PAGE 2	1.35	Km at 17/0
WEST	11	*Would have lower FS than polygon 9, due to lower overall slope angle; so only preliminary analyses run.*	Pre-Development			
WEST	11		Post-Development	20080324141634796.pdf PAGE 2	2.43	Correct head and toe
CENTRAL, N HALF	22		Pre-Development	20080324134701263.pdf PAGE 1	2.42	CONF WATER, LOW LEVEL, ALL STRENGTHS RESIDUAL
CENTRAL, N HALF	22		Post-Development	20080324134701263.pdf PAGE 2	1.71	CUT-AND-FILL SURFACE, CONF WATER, HIGH LEVEL, ALL STRENGTHS RESIDUAL
CENTRAL, N HALF	21	LINES 2-5 v4 cdr9.pdf/ 3/12/2008	Pre-Development	20080325162803509.pdf PAGE 1	1.11	WATER TABLE AT 5500 fps contour; ALL STRENGTHS RESIDUAL except Km, which is near-residual
CENTRAL, N HALF	21		Post-Development	20080325162803509.pdf PAGE 1	1.05	Same as above, but water table is raised 6.8 ft
CENTRAL, QEFY	1	Qefy 6.pdf/ 3/10/2008	Pre-Development	20080324133019103.pdf PAGE 1	1.11	PLANAR model of Qefy only; both UNC water table (W1) and CONF aquifer (W2); all residual strengths
CENTRAL, QEFY	1		Post-Development	20080324152116408	1.07	Same as above, but W1 raised by 7.0 ft
CENTRAL, S HALF	14	Lines C1-C5 x-section 1.pdf/ 1/22/2008	Pre-Development	20080324091907811.pdf PAGE 1	1.08	Uses Resid. 25°/190 psf for Qlso, 17/0 for Km; water table at -22 ft
CENTRAL, S HALF	14		Post-Development	20080324095833788.pdf PAGE 1	1.04	Same as above, but raised water table by 3.5 ft
EAST	36	E Line section 4 with GW rev.pdf/ 2/3/2008	Pre-Development	20080321064357677.pdf PAGE 2	1.11	Wx shale= 12°/260 psf (residual strength); Km = 30/150 (Pk);
EAST	36		Post-Development	20080321064357677.pdf PAGE 1	1.10	Wx shale= 12°/260 psf (residual strength); Km = 30/150 (Pk);

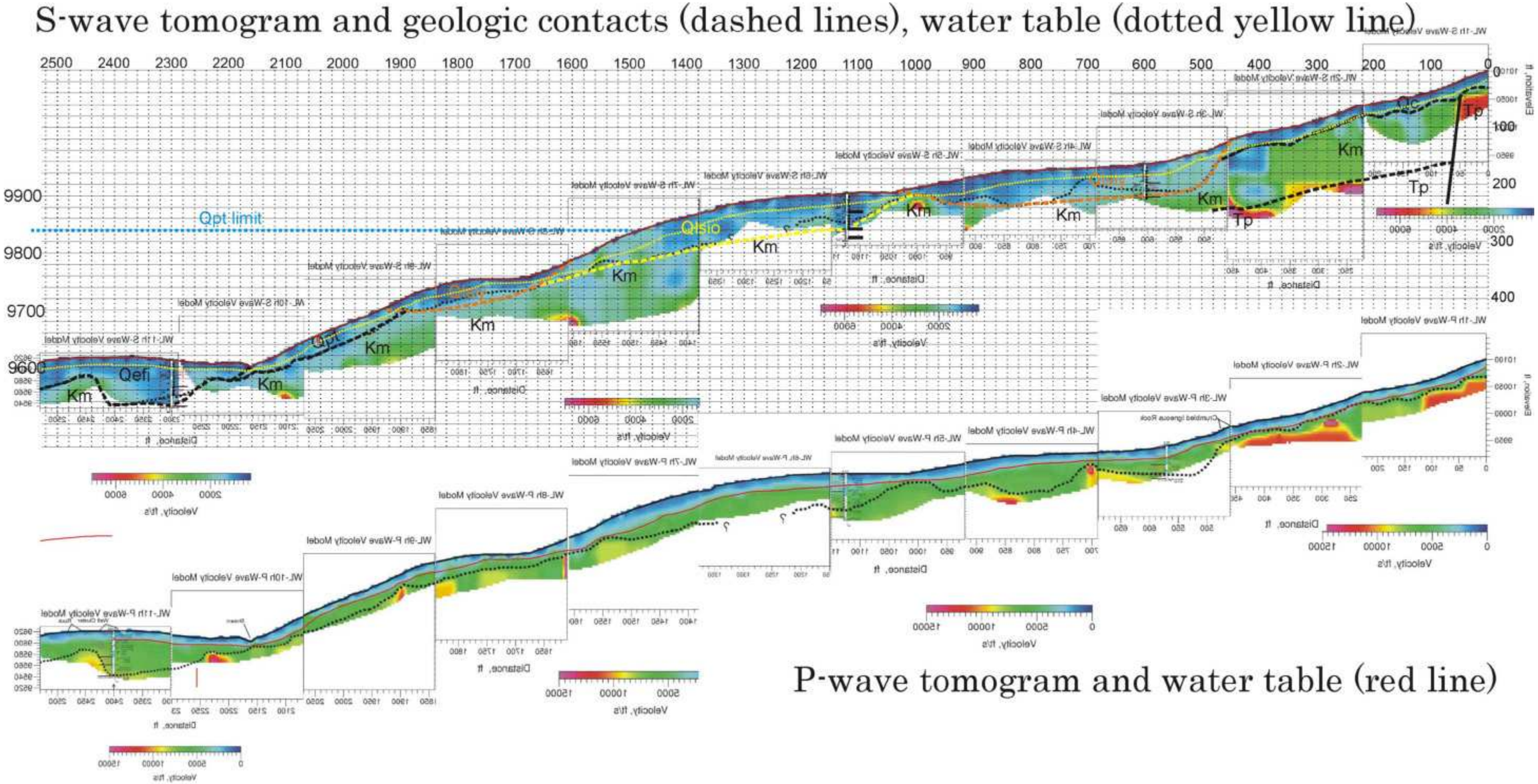

Fig. 8-1. Geologic cross-section of the West Line; NW is to the right. This section was mirrored from the original to put the uphill end at right, to match the stability modeling software. In upper section, background is the S-wave tomogram; velocities are in ft/sec. Geologic contacts are traced between boreholes PZ-13A, -8, and -9 along lines of constant S-wave velocity. In lower section, the background is the P-wave tomogram, from which the water table was interpreted.

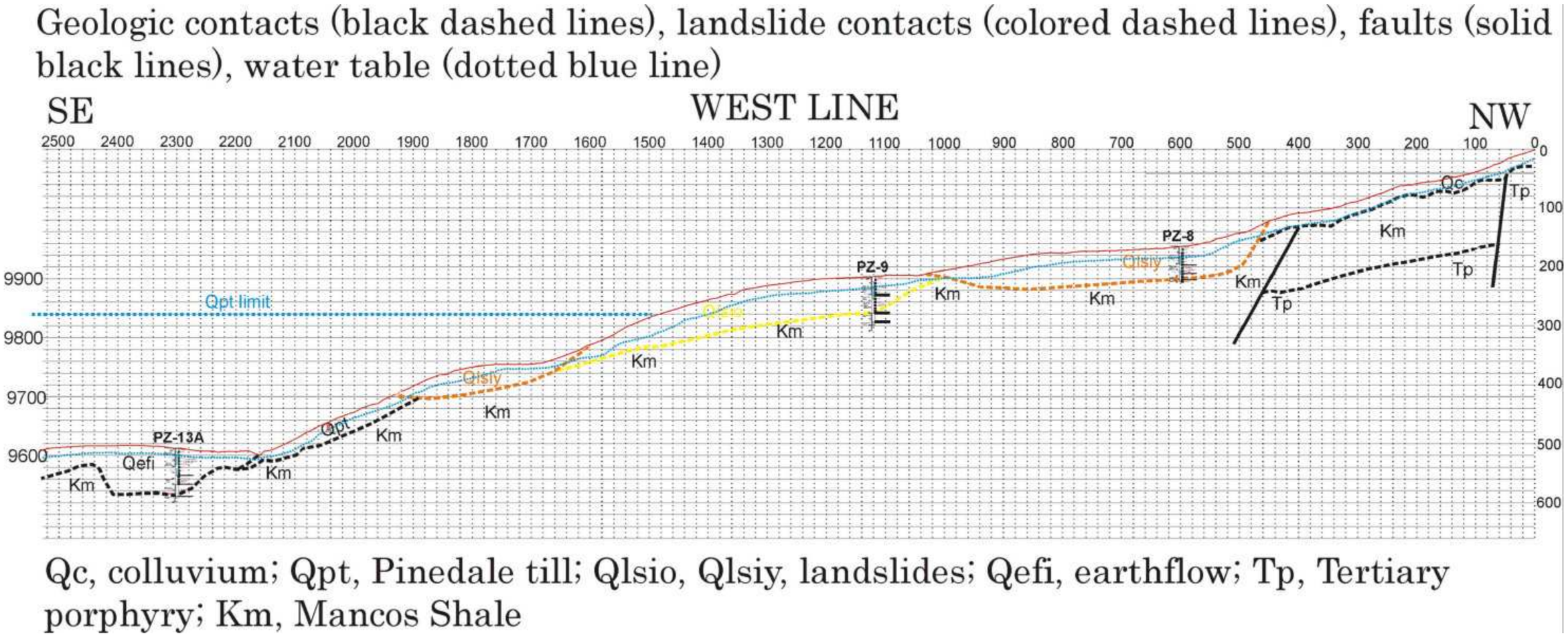

Fig. 8-2. Interpreted geologic cross-section of the West Line, without tomogram background. The water table shown is the pre-development water table. This is the section that was used in the stability analysis.

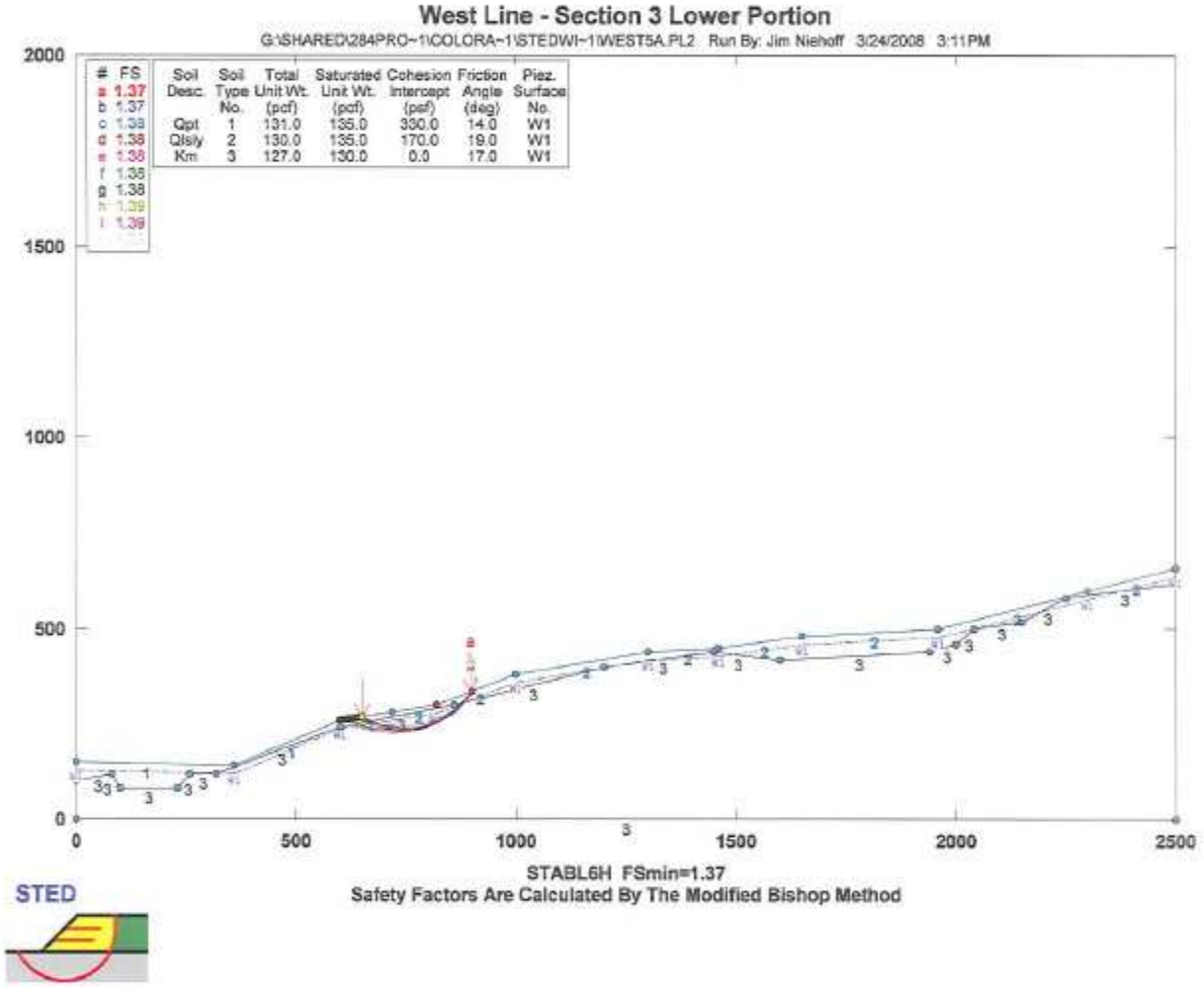

Fig. 8-3. Stability analysis of polygon 9 on the West Section, for **pre-development** conditions. Stability run= **20080324141634796.pdf, PAGE 1.**

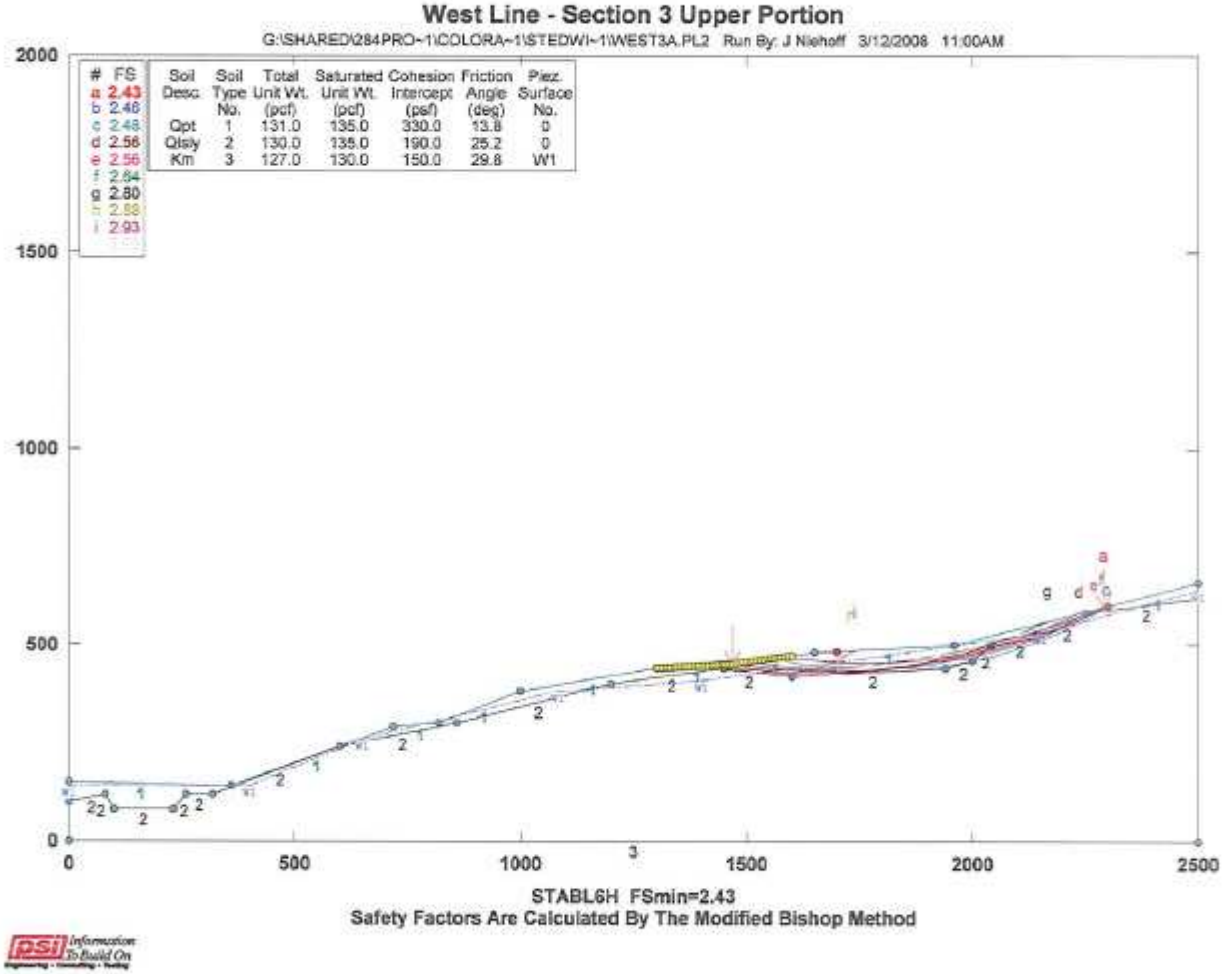

Fig. 8-4. Stability analysis of polygon 11 on the West Section, for pre-development conditions. Because of the high Factor of Safety, and the small (1 ft) predicted rise of groundwater due to development, we did not analyze the post-development stability of this polygon. Stability run= **20080324141634796.pdf, PAGE 1.**

8.3.1.1 Pre-Development Stability

On the West Line we analyzed the stability of the two youngest discrete landslides, polygon 9 on the steep slope band, and polygon 11 near the head of the Line. Polygon 9 shows strong back-rotation of the landslide body, suggesting a strongly curved failure plane. In addition, the material that failed was probably Pinedale till (Qpt) plastered up against a steep Mancos Shale slope eroded by the glacier. Because the till is relatively thin on the steep slope band, any strongly-curved failure plane would penetrate into the Mancos Shale; therefore, we assigned residual strength to the shale, something which we generally do not do on other stability cross-sections.

RESULTS: Polygon 9 has a Factor of Safety of 1.37 for pre-development conditions.

We also analyzed polygon 11 for stability, assuming that both landslide deposits and Mancos Shale were at residual strength. This slide underlies the head of the West Slide Complex, but lies at a much lower average slope angle than does polygon 9.

RESULTS: Polygon 11 has a relatively high Factor of Safety (2.43). This high value reflects the overall low slope angle (8.5°) from the head to toe of this landslide.

8.3.1.2 Post-Development Stability

The upper 1/3 of the West Line lies in sub-watershed A3-8. According to the IAD design of 21-JUN-2007 and Chapter 5, this sub-watershed has a post-development Infiltration Ratio of 1.17 (Appendix 8.1), while the lower 2/3 (including polygon 9) lies in sub-watershed A3-2, which has a post-development Infiltration Ratio of 1.0. The weighted average Infiltration Ratio is 1.06, indicating a 6% increase to groundwater due to the proposed action (Table 8-7). As shown in Fig. 8-1, the unconfined aquifer of the West Line averages about 16 ft thick in polygon 9. Thus, a 6% rise in the water table equates to a 1 ft rise, which is the rise we input for the post-development stability analysis.

RESULTS: Polygon 9 has a Factor of Safety of 1.35 under Post-development conditions. This value is only slightly lower than the pre-development value, because the predicted rise in groundwater after development is only 1 ft. That rise is low, in turn, because the sub-watersheds containing polygon 9 (and uphill of it) have little proposed trail clearing and snowmaking in the 21-JUN-2007 design.

Given the relatively high FS of polygon 11 in pre-development conditions, and the small change due to development, we did not run a post-development analysis of polygon 11.

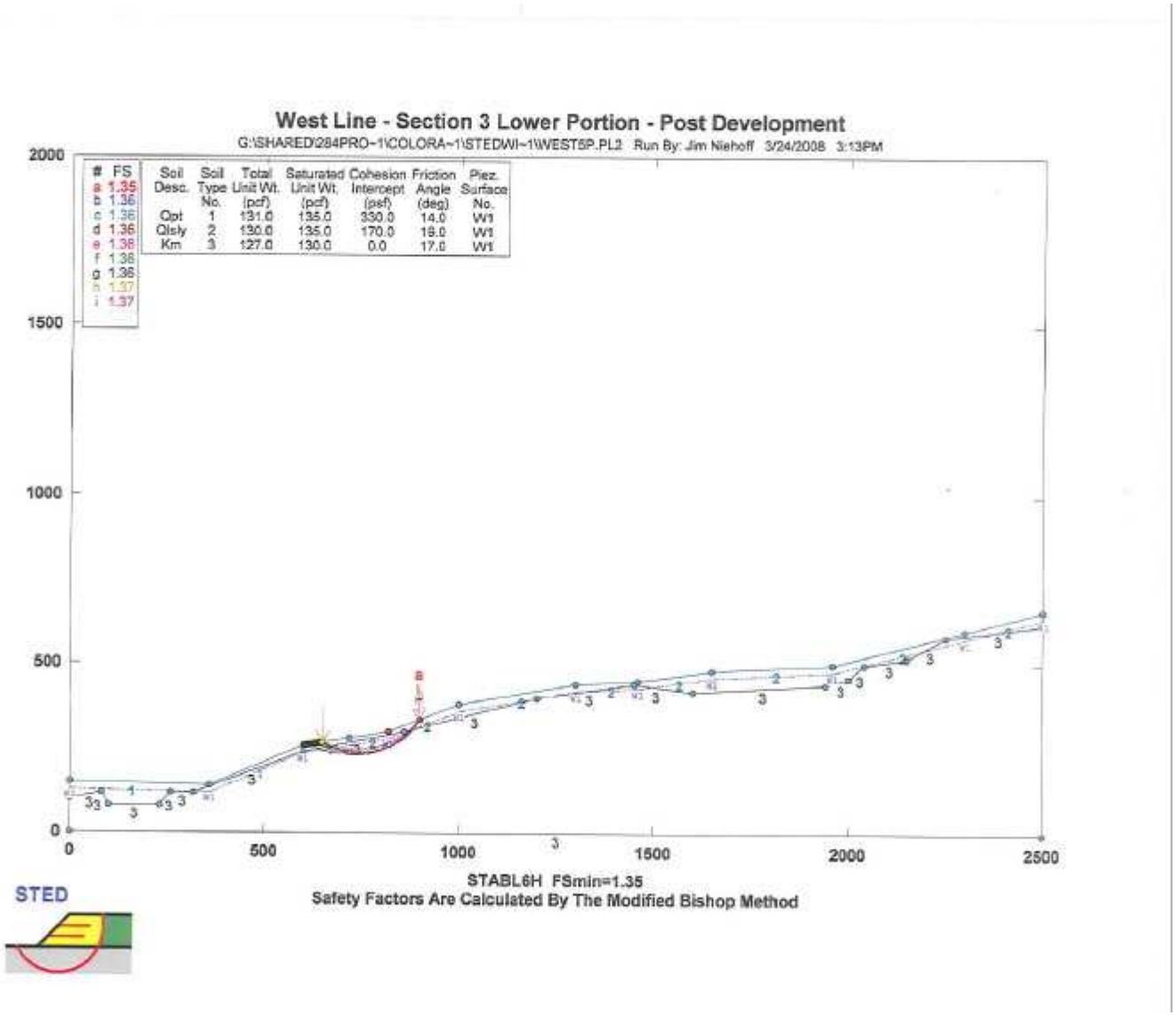

Fig. 8-5. Stability analysis of polygon 9 on the West Section, for post-development conditions. Stability run= **20080324141634796.pdf, PAGE 2.**

Table 8-7. Weighted Infiltration Ratios along the stability cross-sections.

Weighted Infiltration Ratios Along Stability Cross-Sections								**Rise in**
Cross-Section Name	Subbasin Number	Subbasin Begin (ft)	End ft)	% of total length	Subbasin Infiltration Ratio	Weighted Infiltration Ratio	Aquifer Thickness (ft)	**Water Table After Devel**
	A3-5	0	280	0.18	1.34	0.24		
	A3-4	280	380	0.06	1.16	0.07		
	A2-6	380	600	0.14	1.08	0.15		
	C1-5	600	1400	0.51	1.07	0.54		
Central, S half	C1-6	1400	1580	0.11	1	0.11		
				Weighted	Infil Ratio	1.12	29	**3.5**
	A6-3	0	360	0.21	1.28	0.27		
	A4-8	360	590	0.14	1.00	0.14		
	A4-3	590	960	0.22	1.43	0.31		
	A4-2	960	1500	0.32	1.34	0.43		
Central, N half	A4-1	1500	1700	0.12	1.34	0.16		
				Weighted	Infil Ratio	1.30	22.5	**6.8**
	A5-1	0	380	0.21	1.17	0.24		
	A3-9	380	830	0.34	1.27	0.31		
	A3-7	830	980	0.08	1.68	0.14		
	A3-6	980	1420	0.24	1.10	0.26		
	A3-3	1420	1640	0.12	1.02	0.12		
Center, Young Earthflow	A3-4	1640	1850	0.11	1.16	0.13		
				Weighted	Infil Ratio	1.20	15 to 48	**7.0**
	A6-3	0	360	1	1.28	1.28		
Center, Poly 22				Weighted	Infil Ratio	1.28	27	**7.6**
	A3-8	0	770	0.37	1.17	0.43		
	A3-2	770	2090	0.63	1.00	0.63		
West				Weighted	Infil Ratio	1.06	16	**1.0**
East	A4-7	0	180	0.07	1.00	0.07		
	A3-5	180	750	0.22	1.23	0.27		
	C2-2	750	1940	0.45	1.00	0.45		
	C1-2	1940	2640	0.27	1.02	0.27		
				Weighted	Infil Ratio	1.05	26 to 33	**1.3 to 1.7**

8.3.2 Central Cross-Section, North Half

The Central cross-section, North Half, coincides with that part of the Central geophysics Line that lies on and above the steep slope band. The line is 1700 ft long and extends from Ken's Crux/ polygon 22 at the top, to the old earthflow (polygon 27) at the base of the steep slope band (Fig. 8-6). The section is entirely underlain by landslide deposits of the Middle Slide Complex. Bedrock is only exposed at the extreme upslope end (Tp), and, although Mancos Shale presumably approaches near to the surface on the steep slope band (based on outcrops east of the line), Shale is covered along the section line by landslide deposits of polygon 21. The surface morphology is similar to that of the west Section, with the northern 2/3 crossing the low-angle, undulating bench of the Middle Slide Complex, and the southern 1/3 descending 200 ft down the steep slope band.

The geologic contacts on the section (Figs. 8-6, 8-7) were interpreted from the well logs of 3 piezometers (from S to N, PZ-12, PZ-5, and PZ-4) and from the S-wave tomogram (Fig. 8-6). These sources indicate that landslide deposits thicken from about 40 ft thick at the N end of the Middle Slide plateau, to 80 ft at its southern edge. On the steep slope band, landslides deposits thin southward from 50 ft at the crest to 20 ft at the toe (similar to the pattern see on the West Section). The groundwater table was deduced from PZ-8 and -9, along with the 5000 ft/sec contour on the P-wave tomogram.

A possible landslide-related closed depression lies at the head of the steep slope band and just upslope of the polygon 21 headscarp. This depression is on-strike with an apparent graben to the west. From field observations, we deduced that the depression was caused by piping of fine sediments into a tensional opening that lies just upslope of landslide polygon 21. The anomalously thick low-velocity sediments shown on the P-wave tomogram (Fig. 8-6) also suggest highly fractured (dilated) materials here. Our interpretation is that movement of polygon 22 has de-buttressed the crest of the steep slope band at this location, resulting in deep-seated gravitational spreading to the southeast, along pre-existing, NE-striking faults in bedrock. Faults of a similar trend are mapped by Gaskill et al. (1991; see Chapter 2, Fig. 2-5) as cutting the Snodgrass laccolith farther north.

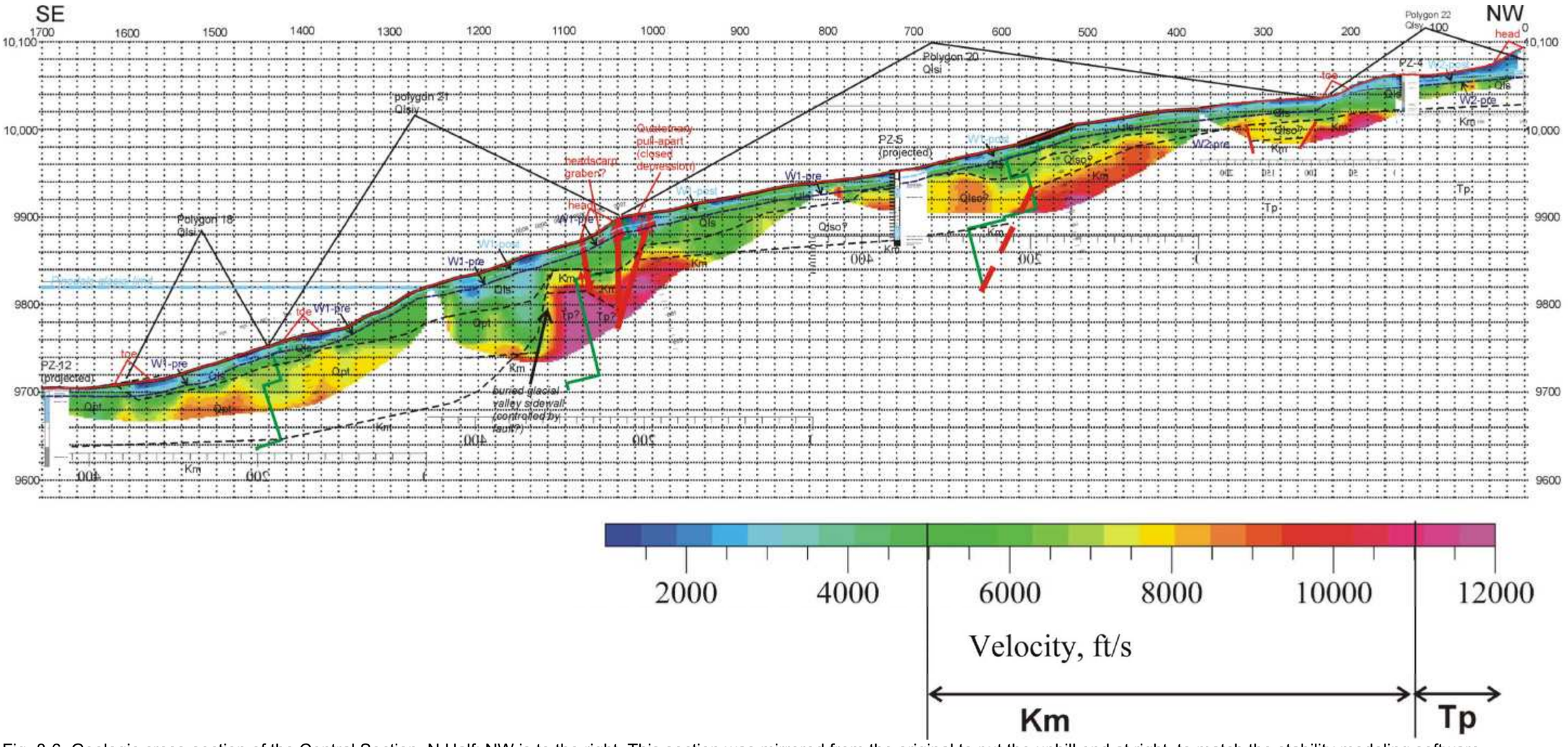

Fig. 8-6. Geologic cross-section of the Central Section, N Half; NW is to the right. This section was mirrored from the original to put the uphill end at right, to match the stability modeling software. Background is the P-wave tomogram; velocities are in ft/sec. Geologic contacts are traced between boreholes PZ-112, -5, and -4 along lines of constant P-wave velocity. Water table was inferred from the highest observed water level observed in the piezometers between Aug. 2007 and Jan. 2008.

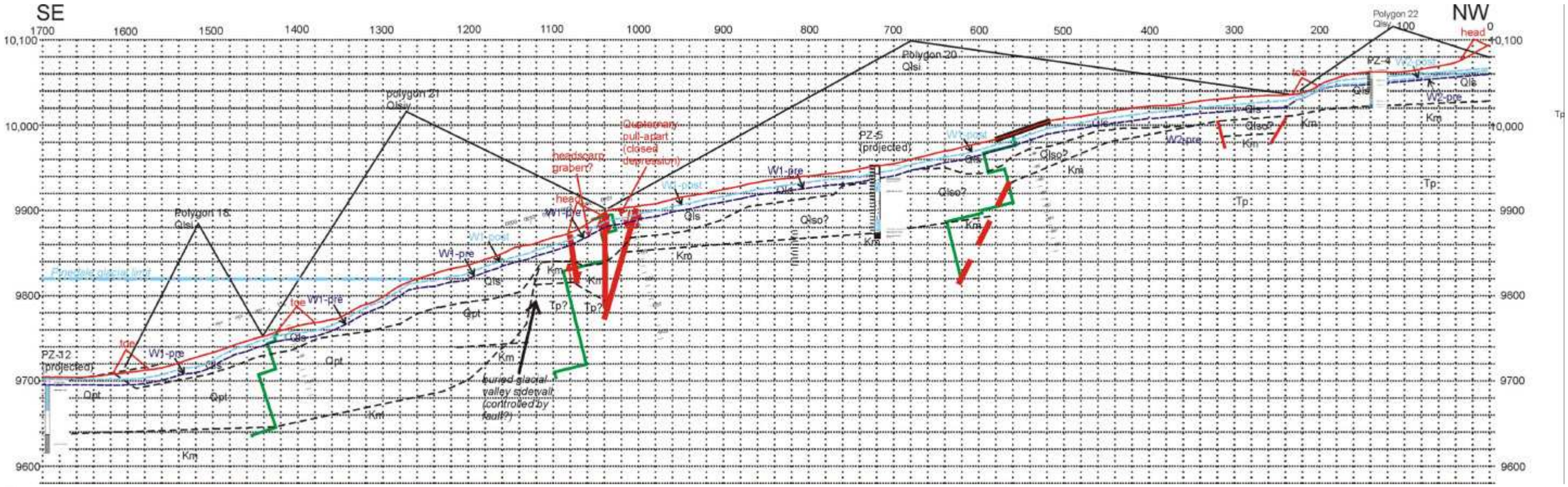

Fig. 8-7. Interpreted geologic cross-section of the Central Section, N Half, without tomogram background. Red lines show inferred faults, probably caused by gravitational spreading rather than by recent tectonics. The water tables shown are the pre-development unconfined water table (W1-pre), based on piezometer data, and the predicted post-development unconfined water table (W1-post), based on the weighted Infiltration Ratio along the section. This is the section that was used in the stability analysis.

8.3.2.1 Pre-Development Stability

On the Central Section, N Half, we analyzed the stability of the two youngest discrete landslides, polygon 22 at Ken's Crux, and polygon 21 on the steep slope band. Polygon 22 is discussed in a separate section. We did not analyze polygon 20, which makes up most of the bench of the Middle Slide Complex, because it is clear that polygon 21 has a much steeper slope and would fail well before polygon 20 would fail.

Below, we describe the stability of polygon 21, the topography of which shows evidence for weak back-rotation of the landslide body, suggesting a shallow but curved failure plane. In addition, the material that failed was probably Pinedale till (Qpt) plastered up against a steep Mancos Shale slope eroded by the glacier, just as on the steep slope band of the West Section (polygon 9). Because the till here is roughly twice as thick (40 ft) as the till on the West Section, the failure plane may not have penetrated into the Mancos Shale; therefore, we ran simulations with the Mancos Shale at peak strength (corresponding to a 40 ft-thick landslide that does not involve shale bedrock) and at residual strength (corresponding to a deeper landslide with a failure plane in Mancos Shale).

RESULTS: Polygon 21 has a Factor of Safety of 1.11 for pre-development conditions. Given the assigned residual strengths and the location of the existing water table, the low-FS failure planes remain within the thick Pinedale till on the steep slope band, and do not penetrate down into shale bedrock.

8.3.1.2 Post-Development Stability

The Central Section, N Half crosses five sub-watersheds (see Chapter 5). According to the IAD design of 21-JUN-2007 and Chapter 5, the weighted average Infiltration Ratio along the section is 1.30, indicating a 30% increase to groundwater due to the proposed action. This relatively high increase reflects the trail clearing and snowmaking through Ken's Crux and down to the lift terminals at the base of the steep slope band. As shown in Fig. 8.3, the unconfined aquifer of the West Line ranges from 15-30 ft thick (average 22.5 ft thick) in polygon 21. Thus, a 30% rise in the water table equates to a 6.8 ft rise, which we have rounded up to 7 ft as the rise we input for the post-development stability analysis.

RESULTS: Polygon 21 has a Factor of Safety of 1.05 under Post-development conditions. This value is lower than the pre-development value, because the predicted rise in groundwater is 7 ft. That rise is high, in turn, because the sub-watersheds containing the stability section have extensive proposed trail clearing and snowmaking in the 21-JUN-2007 design. As will be discussed in Chapter 9, this low stability will have to be mitigated by lowering the water table on the steep slope band, via a combination of interceptor ditches and horizontal drains.

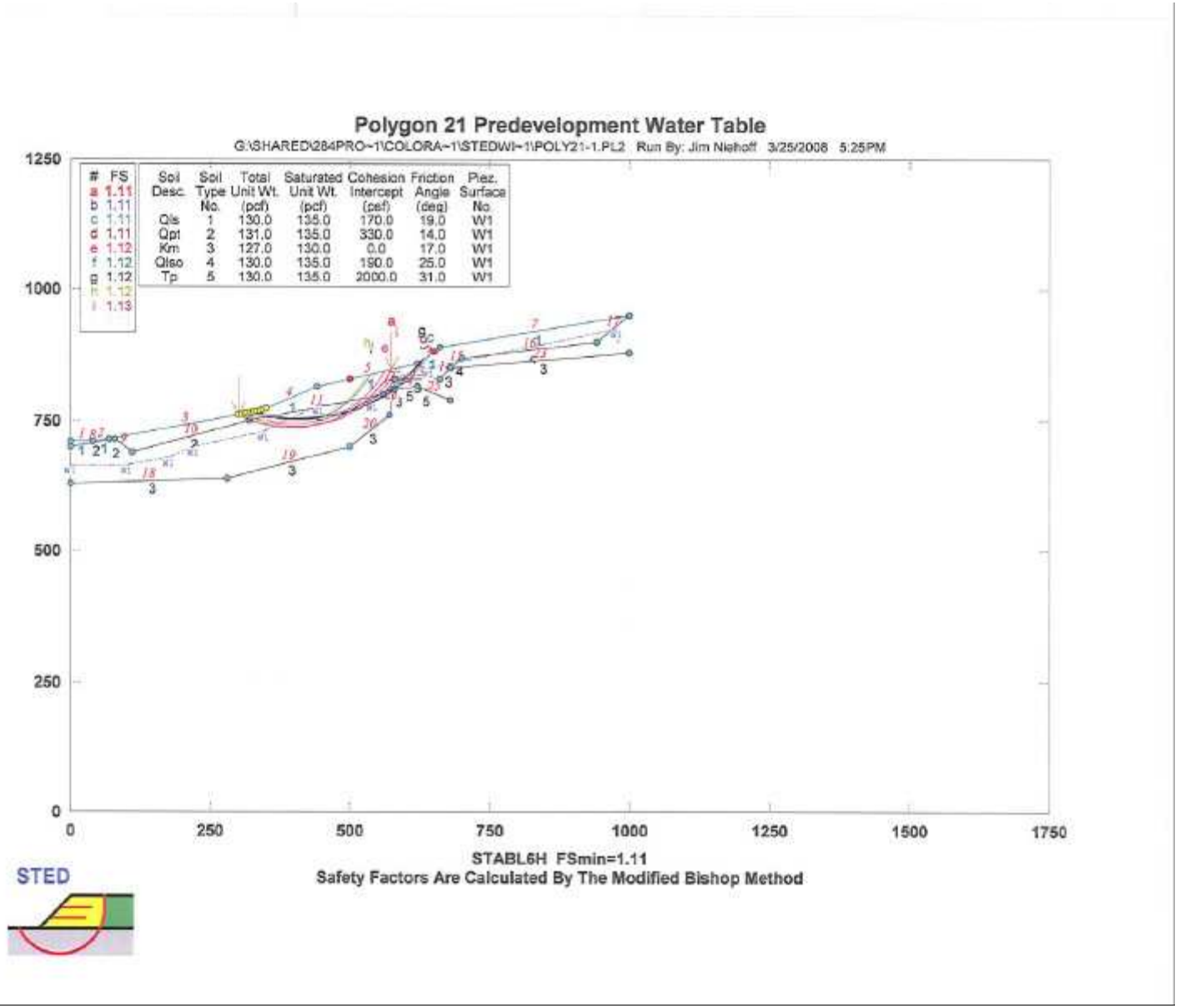

Fig. 8-8. Stability analysis of polygon 21 on the Central Section, N Half, for pre-development conditions.

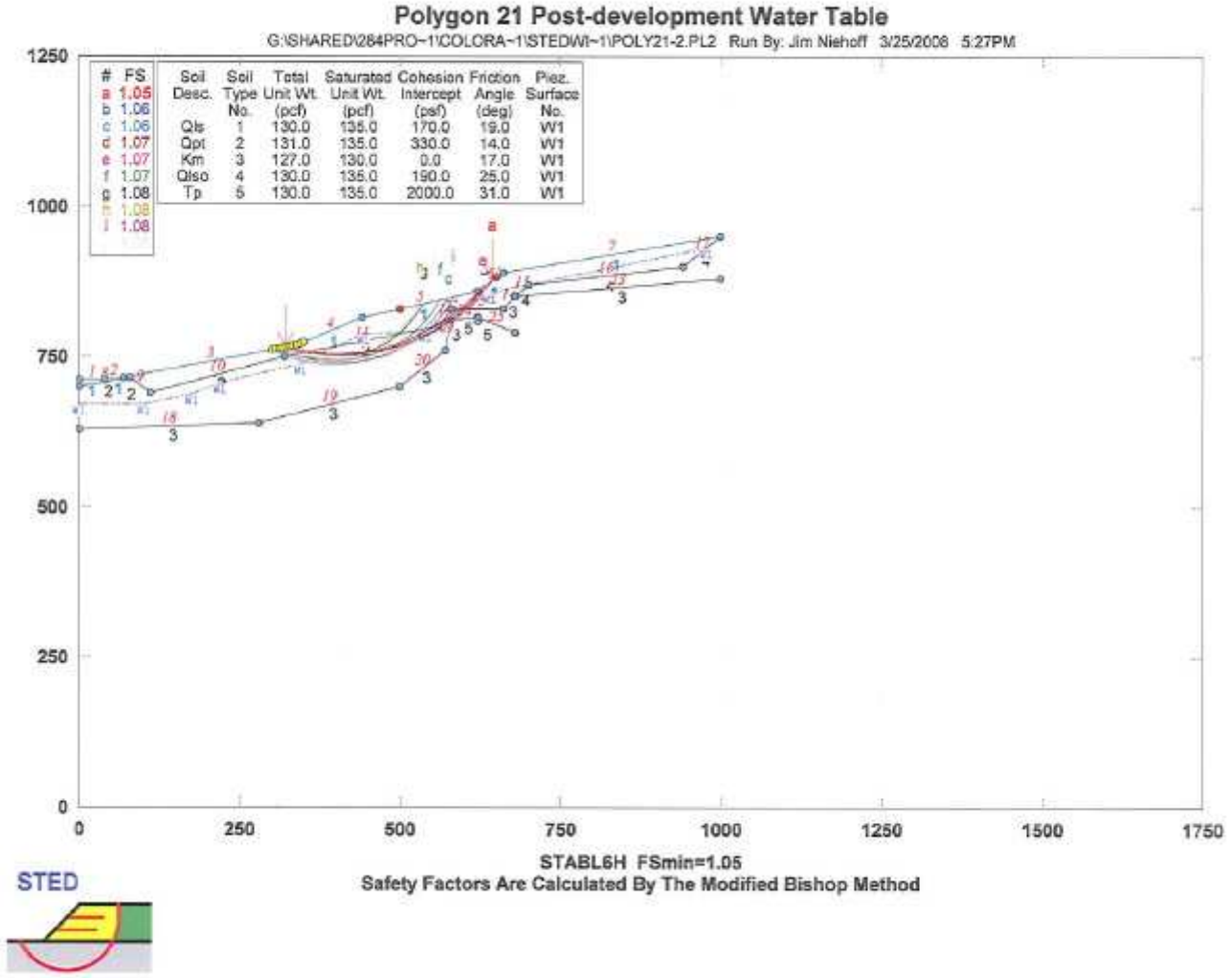

Fig. 8-9. Stability analysis of polygon 21 on the Central Section, N Half, for post-development conditions.

8.3.3 Central Cross-Section, South Half

The Central cross-section, South Half, coincides with that part of the Central geophysics Line that lies below (south of) the steep slope band, and thus, below the Pinedale glacial trimline. The line is 1600 ft long and extends from the old (lower) earthflow (polygon 27) at the foot of the steep slope band, across the Slump Block of Baum (1996), and downhill to the nearly flat terrain at the foot of Snodgrass Mountain (Fig. 8-10). The section is underlain by thick glacial till on the Slump Block (more than 117 ft thick at PZ-14; Mancos Shale was not reached), and by earthflows and landslides composed mainly of reworked till of more than one age. No Mancos Shale or porphyry bedrock is exposed in the section. The surface morphology is dominated by low, parallel, bouldery ridges of till on the Slump Block, which grade downslope into landslide-related scarps.

The geologic contacts on the section (Figs. 8-10, 8-11) were interpreted from the well logs of 3 piezometers (from S to N, PZ-15, PZ-14, and PZ-12) and from the S-wave tomogram (Fig. 8-10). These sources indicate that depth to bedrock ranges from 140 ft (beneath the Slump Block and head of polygon 14), to 80 ft beneath the old (lower) earthflow, to 35-50 ft at the toe of the slope and beneath the level surface of polygon 12. These depths are 2-3 times greater than typical depths to bedrock above the steep slope band, and indicate that Pinedale (and older) glaciers had deposited a considerable thickness of till below the slope band. Some of the Quaternary stratigraphic section may be old landslide deposits from Snodgrass Mountain intercalated between till sheets. The groundwater table was deduced from the piezometers, along with the 5000 ft/sec contour on the P-wave tomogram.

8.3.3.1 Pre-Development Stability

The most unstable landslide on this section (based on overall slope angle) is polygon 14, which lies on the southern edge of the Slump Block (Fig. 8-10). The surface morphology displays a moderate amount of back-rotation, suggesting a moderately deep circular failure arc. Because the depth to bedrock is averages about 80 ft in polygon 14, most of the failure plane is probably restricted to within the till or underlying old landslide deposits, so we use residual strength for both those materials. The failure plane may reach the top of Shale near the toe, at which point it cuts across shale bedding and is assigned a near-residual strength (17°/0 psf).

RESULTS: Polygon 14 has a Factor of Safety of 1.08 under Pre-development conditions. This value represents a conservative estimate, since all strengths were assumed to be residual, as well as other conservative assumptions as outlined in Sec. 8.2.4.5.

8.3.3.2 Post-Development Stability

On this section, the unconfined aquifer ranges from 19 ft thick (-26 to -45 ft) at PZ-15, to 39 ft thick (-26 to -65 ft) at PZ-14, to 30 ft thick (-10 to -40) at PZ-12. Thus the mean aquifer thickness is 29 ft. The weighted Infiltration Ratio is 1.12, which implies a water table rise of 3.4 ft due to development.

RESULTS: under the post-development water table, the Factor of Safety is 1.04, assuming conservative input values.

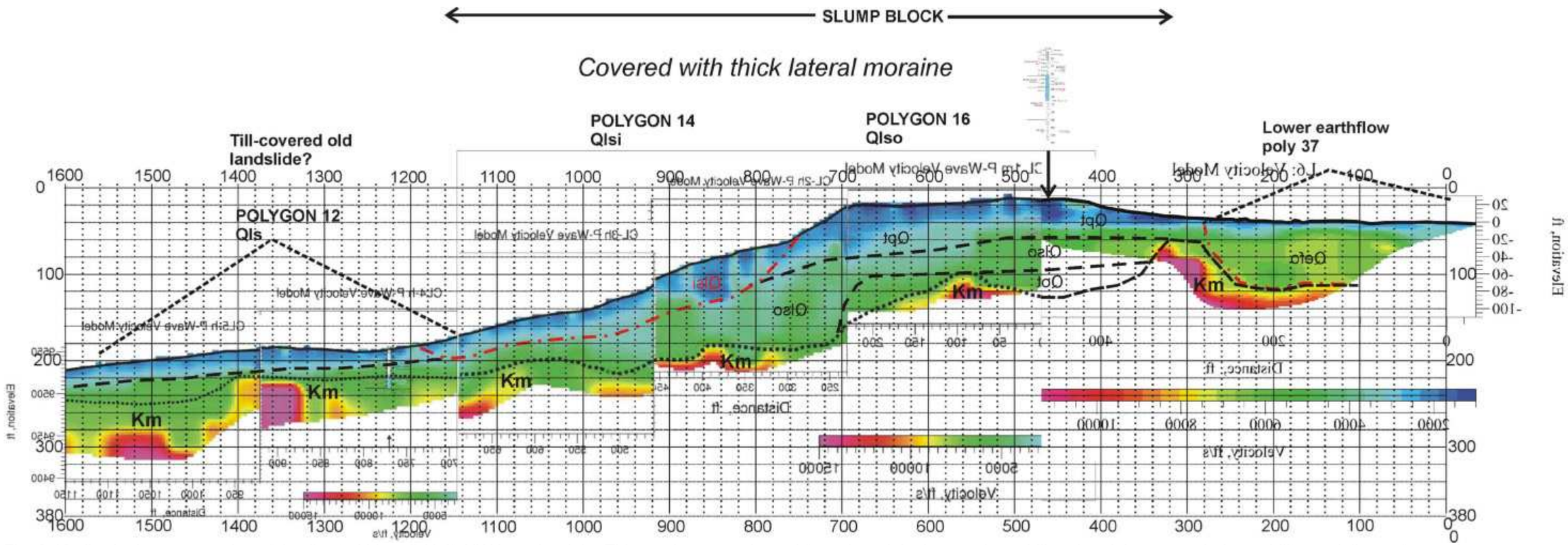

Fig. 8-10. Geologic cross-section of the Central Line, S Half; NW is to the right. This section was mirrored from the original to put the uphill end at right, to match the stability modeling software. In upper section, background is the S-wave tomogram; velocities are in ft/sec. Geologic contacts are traced between boreholes PZ-13A, -8, and -9 along lines of constant S-wave velocity. In lower section, the background is the P-wave tomogram, from which the water table was interpreted.

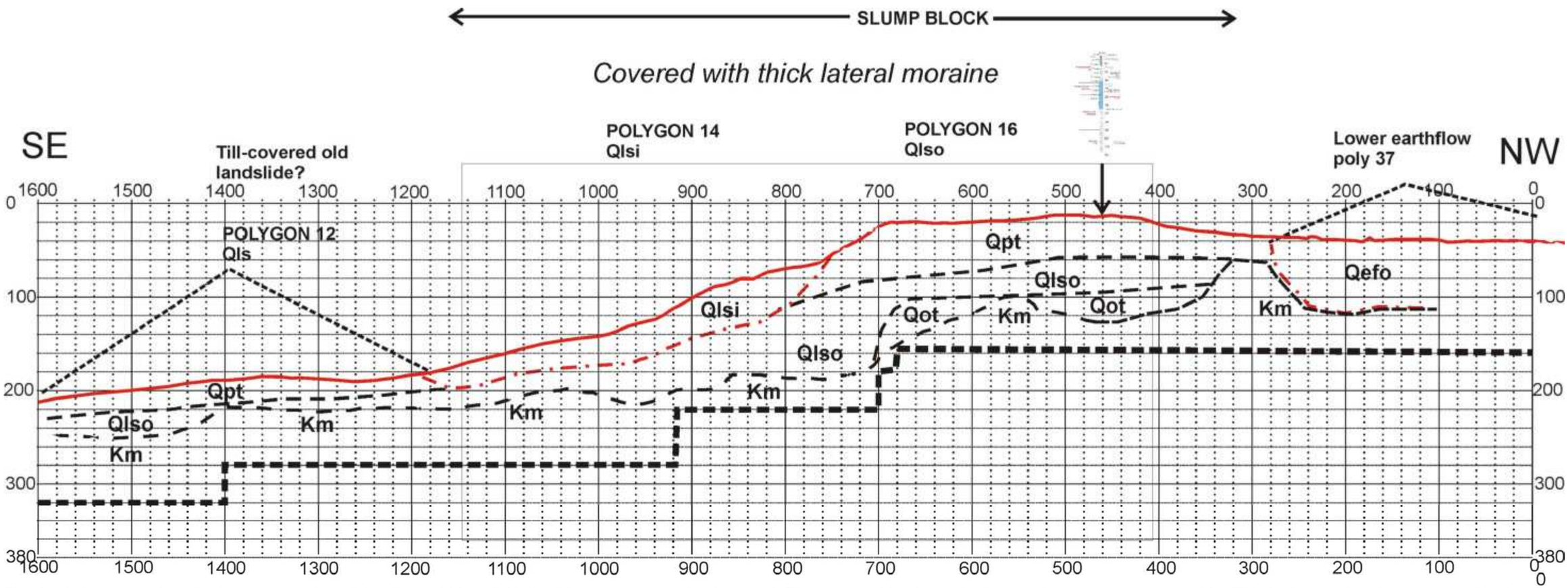

Fig. 8-11. Interpreted geologic cross-section of the Central Line, S Half, without tomogram background. The water table shown is the pre-development water table. This is the section that was used in the stability analysis.

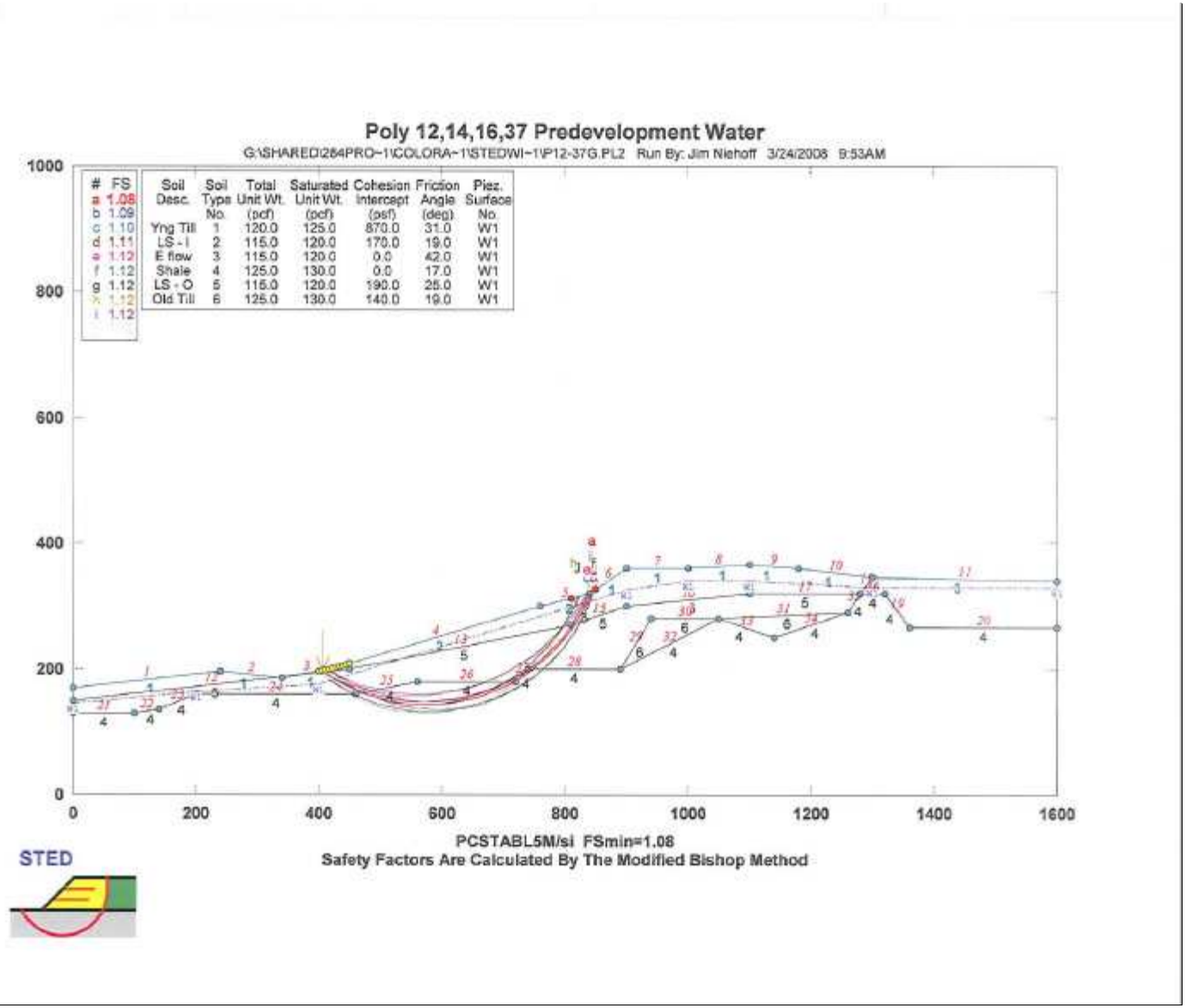

Fig. 8-12. Stability analysis of polygon 14 on the Central Section, S Half, for pre-development conditions.

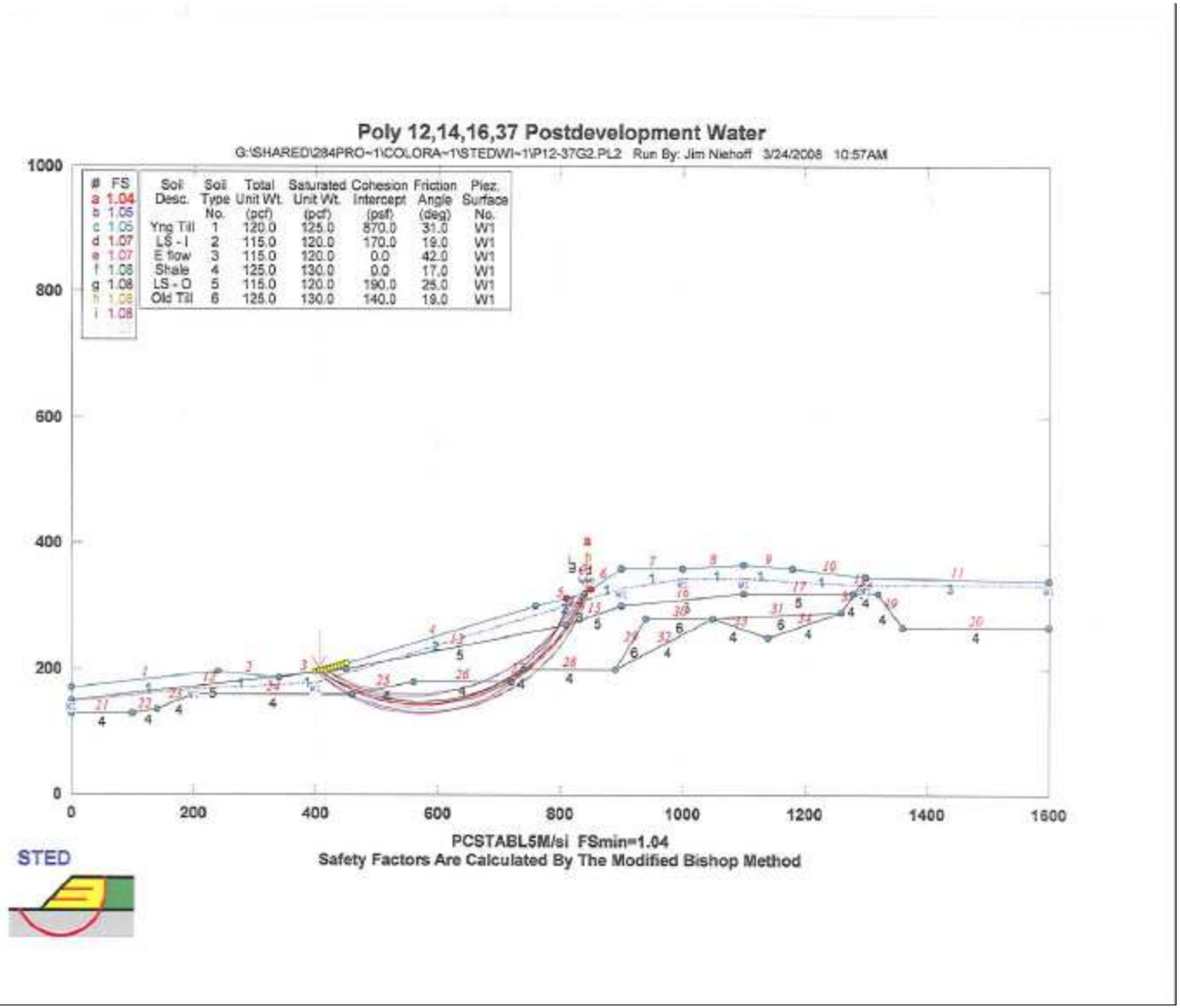

Fig. 8-13. Stability analysis of polygon 14 on the Central Section, S Half, for post-development conditions.

8.3.4 Ken's Crux landslide (polygon 22)

The Ken's Crux landslide comprises the northernmost 360 ft of the Central Section, N Half, and lies directly SE of Ken's Crux. The landslide is a small, young-looking slump (Qlsy) about 225 ft long and 200 ft wide, with an L-shaped headscarp. The headscarp exposes an in-situ Tertiary porphyry sill of the transition zone near Ken's Crux. The surface morphology is that of a simple, monolithic rotational slump block. This landslide is significant because a trail with snowmaking must be placed on its western edge, along with a snowmaking water pipeline, and some fill derived from grading the headscarp downward at its extreme west end.

The geologic contacts on the section (Figs. 8-14, 8-15) were interpreted from the well logs of piezometer PZ-4 and from the P-wave tomogram (Fig. 8.14). These sources indicate that depth to bedrock is 38 ft beneath the center of the slide.

The groundwater table was deduced from PZ-4, which revealed a very thin (4 ft thick) confined aquifer overlying Mancos Shale at 38-42 ft BGS. Water in this aquifer rose up to within 14 ft of the ground surface after drilling, a rise of 24 ft, indicating strongly confined conditions.

8.3.4.1 Pre-Development Stability

The pre-development stability of the Ken's Crux slump was analyzed by assigning the strong confined pore pressure to the Mancos Shale beneath the landslide deposit. We used a Bishop semicircular trial failure plane restricted to daylight at the topographic head and toe of the slide. Due to the strongly-rotated appearance of the slump block, we assigned near-residual strength to Km, and residual strength to Qlsy.

RESULTS: The Factor of Safety for pre-development conditions, including a strongly confined aquifer atop bedrock, is 2.42. This high safety factor results from the very low slope angle of this slump block.

8.3.4.2 Post-Development Stability

The topography of the western part of the slump block, just west of our cross-section line, will be regarded for ski traffic. This regarding will involve excavating part of the headscarp, putting a fill prism on the head of the slide, cutting the upper part of the toescarp, and filling the toe of the toescarp. In addition, the water table must rise 15%, or as much as 7.6 ft, depending on the total thickness of the aquifer in polygon 22. The net effect of these two actions is to decrease the Factor of Safety from 2.42 to 1.71.

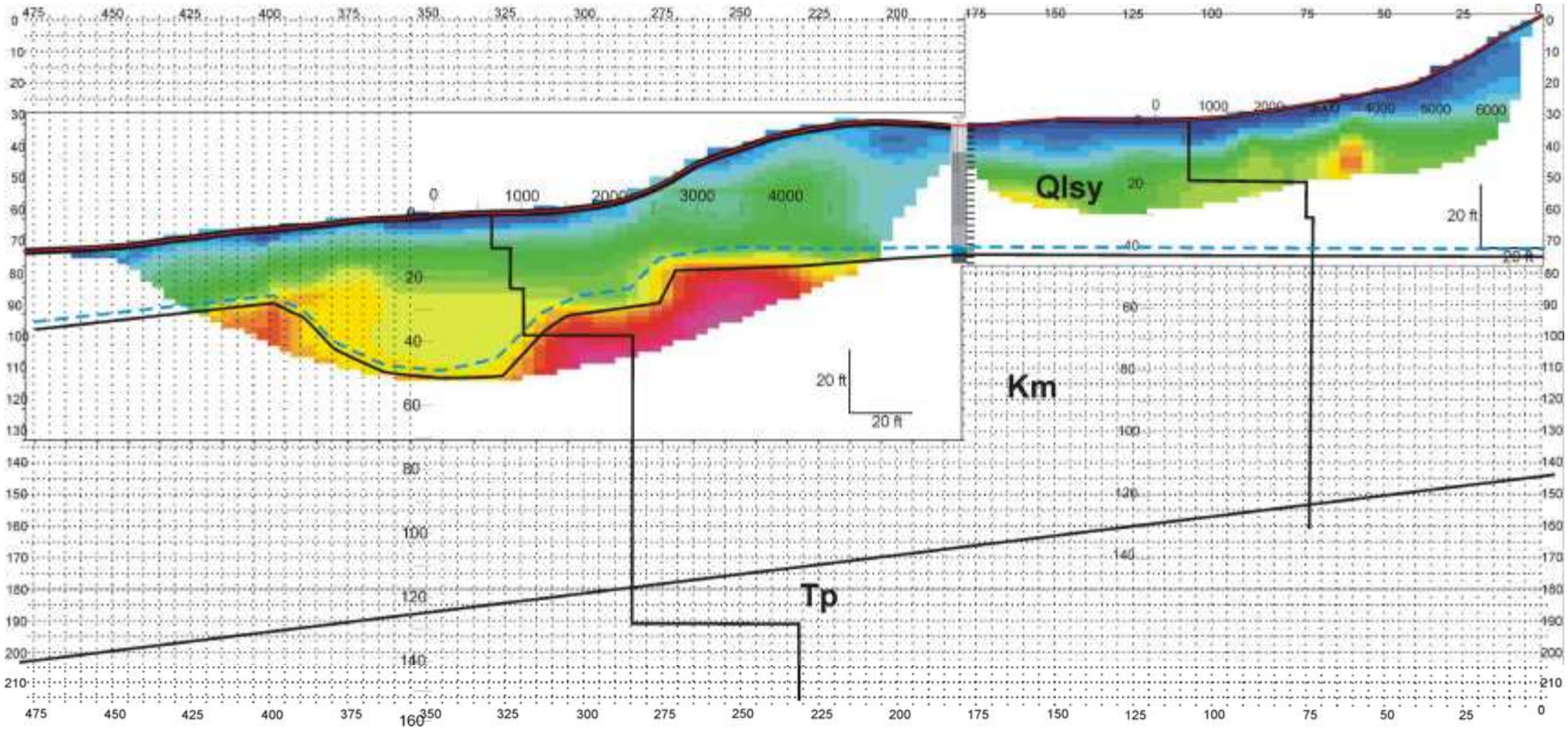

Fig. 8-14. Geologic cross-section of the Ken's Crux landslide, polygon 22; NW is to the right. Background is the P-wave tomogram from Jim O'Donnell; stair-step black lines show S-wave soundings from ReMi, with velocities in ft/sec. Due to the small size of this slump, geologic contacts are controlled only by a single borehole at center (PZ-4), the P-wave tomogram, and the headscarp and toescarp. An inclinometer (I-4) is adjacent to PZ-4, but its hole was not logged.

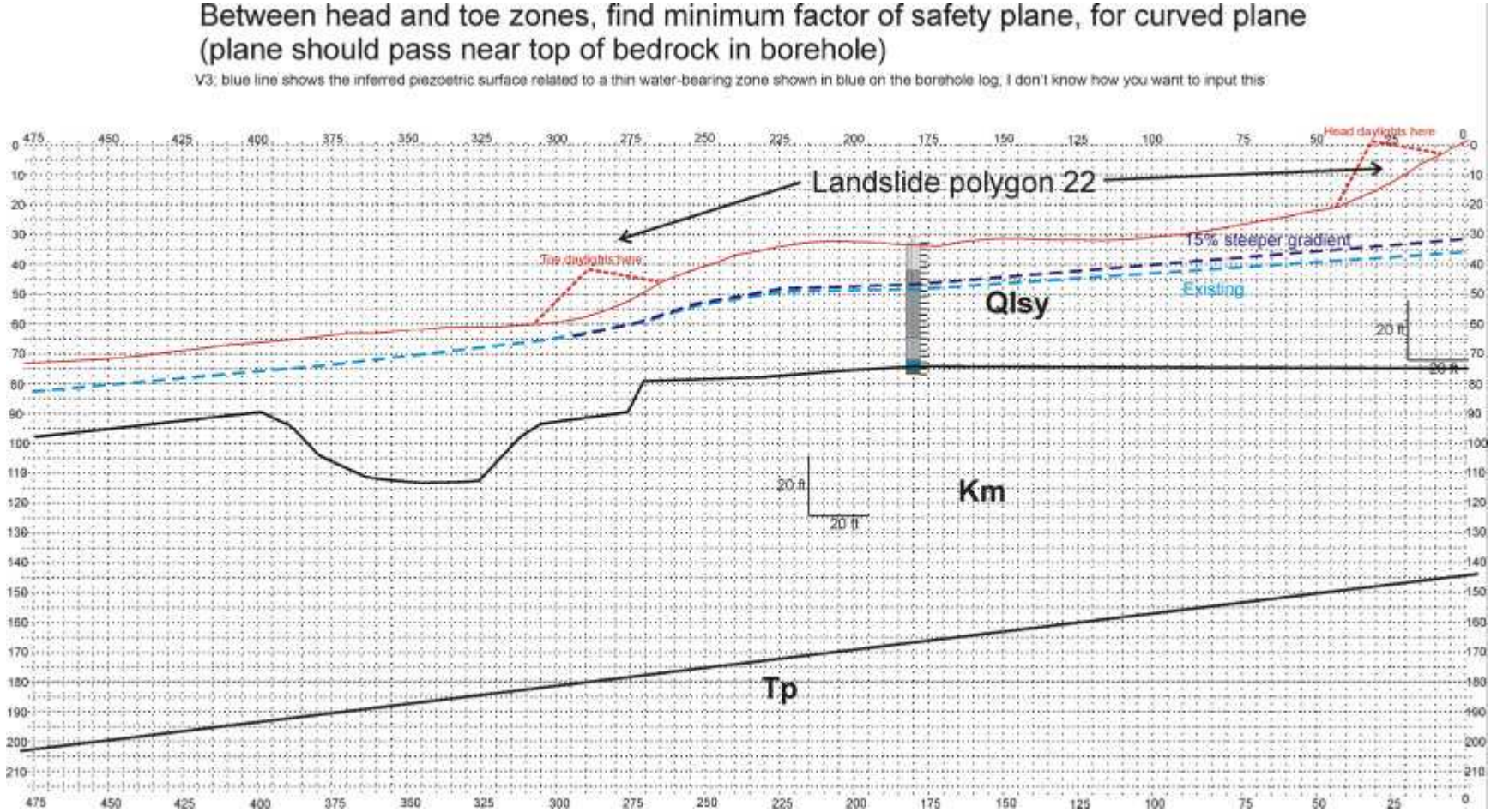

Fig. 8-15. Interpreted geologic cross-section of the Ken's Crux slump, without tomogram background. PZ-4 (at center) shows a strongly confined aquifer only 4 ft thick perched atop bedrock. The piezometric surfaces shown are existing pre-development (light blue dashes) and post-development which is 15% steeper (dark blue dashes). This is the section that was used in the stability analysis.

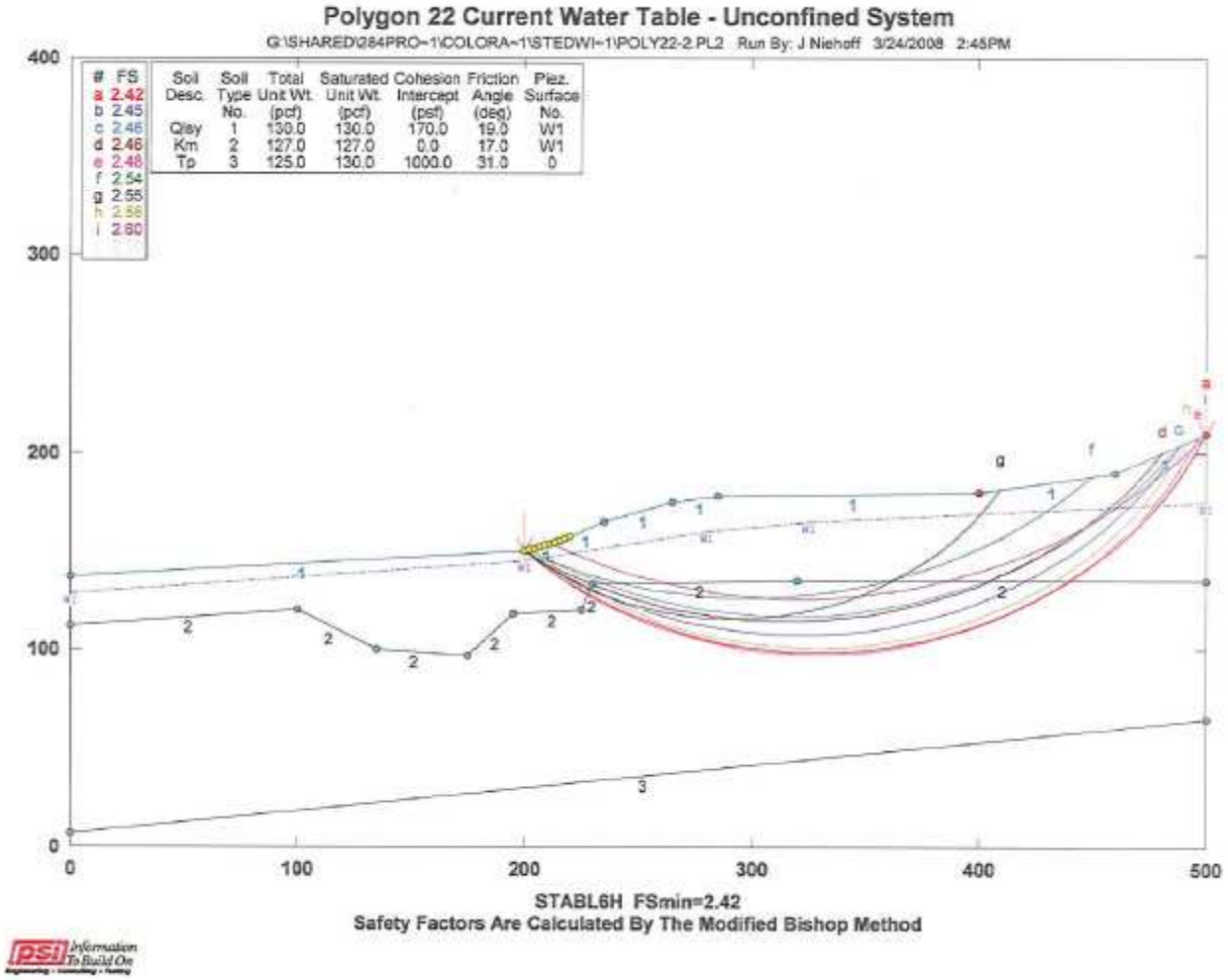

Fig. 8-16. Stability analysis of Ken's Crux slump (polygon 22), for pre-development conditions.

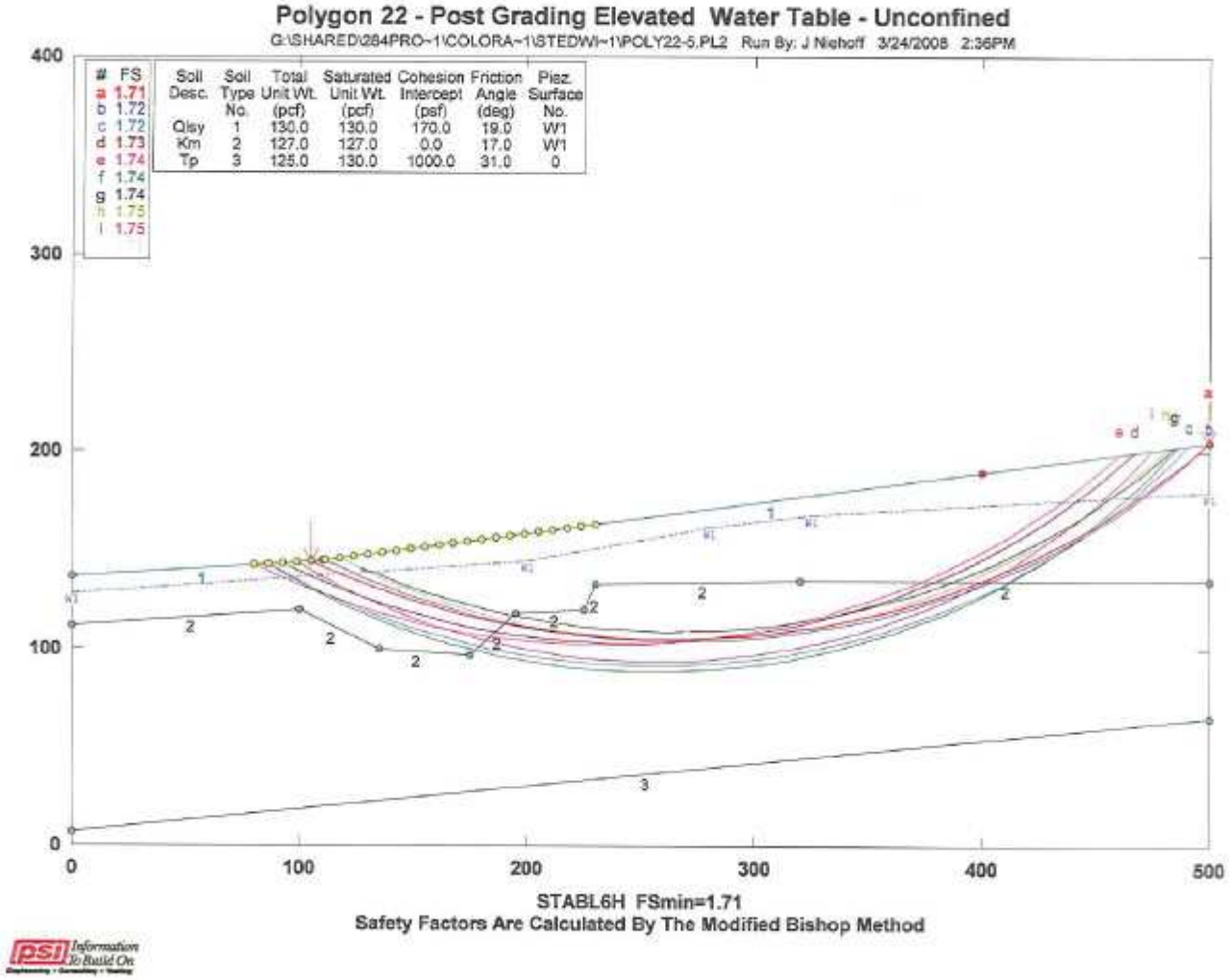

Fig. 8-17. Stability analysis of Ken's Crux slump (polygon 22), for post-development conditions.

8.3.5 Young Earthflow (polygon 1)

The young earthflow (polygon 1, Qefy) lies directly west of the axial stream, and is about 1700 ft long and 220-350 ft wide. The upper 2/3 of the earthflow (Qefi and Qefiy) lies above the steep slope band, whereas the lower 1/3 (Qefy) flows over the steep slope band. The latter displays the youngest-looking transverse scarps and benches. The toe of Qefy lies on the old earthflow (polygon 27) at the base of the steep slope band, and widens to 500 ft wide, like the toe of a piedmont glacier. The lower part of Qefy has a pronounced steep section between 9725-9800 ft, which corresponds to the steep basal section of the steep slope band where Km outcrops (Fig. 8-18). We infer that Qefy here has flowed over the buried glacial-cut cliff in Km, with the toe protruding up to 180 ft out from the base of the original cliff-line.

The cross-section is controlled only by two boreholes (PZ-6A, -6B); no geophysical survey was performed here. Borehole PZ-6A reached Mancos Shale at a depth of 81 ft, overlain by “silty clay and cobbles, some gravel” (from 9-46 ft), “ clay and sparse small cobbles” (46-65 ft), and “clay and scattered boulders” (65-81 ft). The uppermost layer is interpreted as young-intermediate (Qefiy) earthflow deposits, and the basal bouldery layer (distinguished as Qefb) could be pre-Pinedale till or coarse alluvium. Unit Qefb also coincides with a confined aquifer (W2) that has an artesian head roughly 3 ft above the ground surface. A higher unconfined aquifer (W1) exists in the overlying unit Qefiy, which had a seasonal high water table in PZ-6B of -17 ft BGS and is 48 ft thick (down to top of Qefb).

8.3.5.1 Pre-Development Stability

We drew the earthflow/Km contact on the cross-section by extending the contact in PZ-6A, but bringing it up to the surface at the head and toe, and making the earthflow deposit thin as it flowed over the buried glacial-cut cliff (8-18). Likewise, we extended aquifers W1 and W2 laterally, but pinched out the confined aquifer (Qefb) W2 at the oldest, uppermost earthflow unit (Qefiy), and at the head of Qefy. Our reasoning is that the permeable boulder layer is a stratigraphic deposit (possibly old alluvium from an ancestral axial stream) that would probably have been disrupted and destroyed as a continuous layer, by the flow and thinning of the postglacial flow of Qefy over the buried glacial-cut cliff.

We did not interpret a zone of weathered shale here, because neither PZ-6 (in the earthflow) or PZ-5 (across the creek from PZ-6) showed such a zone. Although generally we do find such a zone above the Pinedale glacial limit, we infer that near the axial stream, periodic stream erosion removed the weathered shale zone.

For the earthflow material properties, we used residual friction of 23° and cohesion of 0 psf for Qefy, and 25/0 for Qefb. Mancos Shale was assumed to be at residual strength (10.5/0).

RESULTS: The minimum pre-development factor of safety is 1.11.

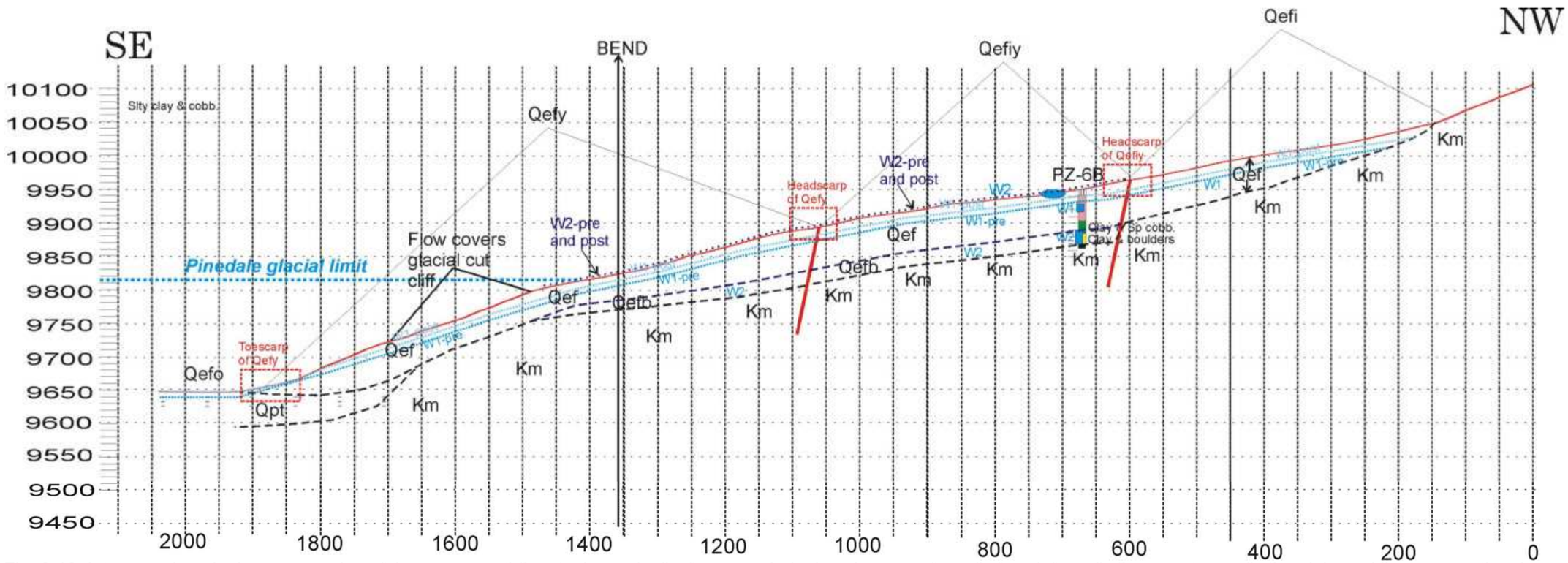

Fig. 8-18. Interpreted geologic cross-section of the young earthflow (polygon 1). Surface morphologic units range from Qefy at left, to Qefiy at center, to Qefi at right; red lines separating the age classes of landslides are not faults, but mark the inferred location of each headscarp. Underlying landslide deposits (Qef) are not differentiated as to age. Instead, we use average density and strength data from earthflow deposits of several ages. For unit Qefb, for which we have no test samples, we arbitrarily increased the density by xx pcf and the friction angle by 5 degrees, to account for the effect of abundant boulders and permeable matrix. The Pinedale glacial limit crosses the earthflow at ca. 9825 ft elevation, and below it, the earthflow is interpreted as flowing over a buried, glacier-eroded cliff in Mancos Shale. PZ-6A (at right center) shows a strongly confined aquifer in a bouldery layer perched atop bedrock. The piezometric surfaces shown are: dark blue dots labeled W2, pre- and post-artesian head of confined aquifer; medium blue dots, labeled W1-pre, pre-development unconfined water table; light blue dots, labeled W1-post, post-development unconfined water table. This is the section that was used in the stability analysis.

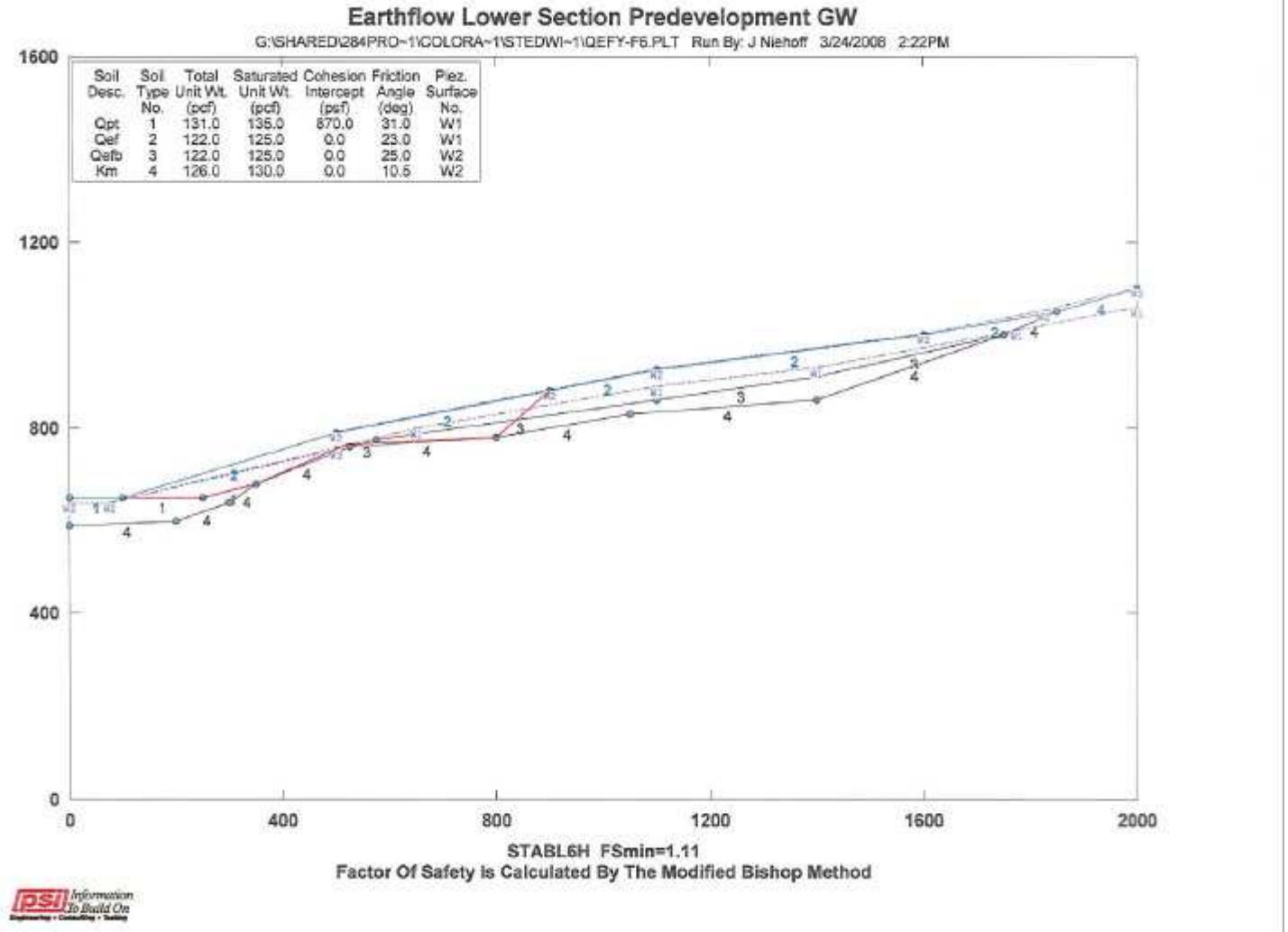

Fig. 8-19. Stability analysis of the Young Earthflow (polygon 1), for pre-development conditions.

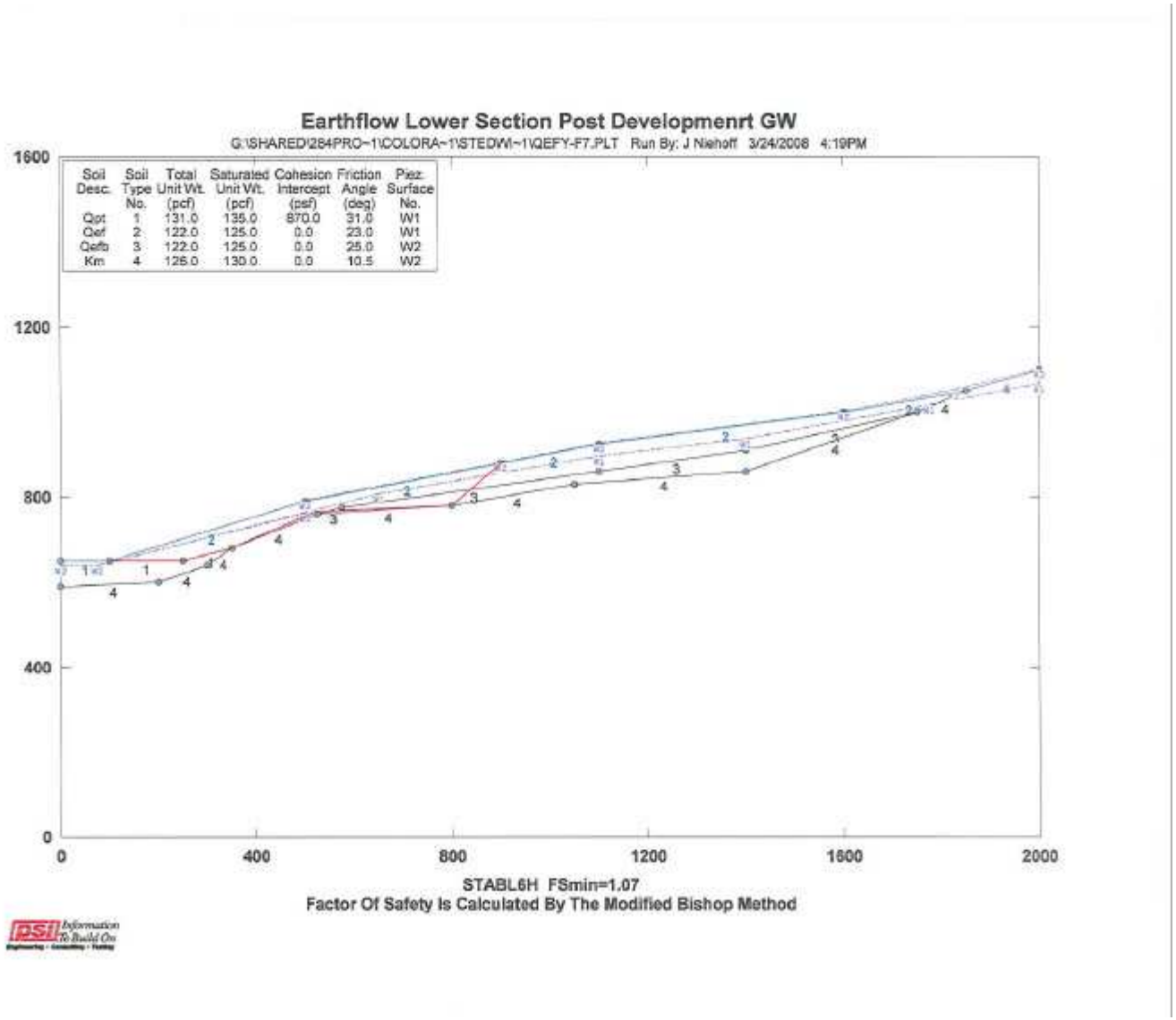

Fig. 8-20. Stability analysis of the Young Earthflow (polygon 1), for post-development conditions.

8.3.5.2 Post-Development Stability

Predicting the post-development piezometric surface(s) in Qefy is difficult, for several reasons. First, there is an upper unconfined and lower confined aquifer, the latter with artesian pressures above the ground surface. It is unclear how the increased moisture from development will be partitioned between these two aquifers. Second, the unconfined aquifer is hydraulically connected to t he axial stream (Chapter 7, Figs. 7-3, 7-4), since it rose due to Fall storms, making it unlike the unconfined aquifers considered in other stability sections.

The weighted Infiltration Ratios suggest that the Qef section will undergo a 20% increase in moisture due to the proposed action. In contrast, the increase in streamflow in the axial stream, which runs down the length of Qefy, is predicted to be 15% (Upper Flume site, stream node A6; see Chapter 5, Table 5.5). Therefore, without knowing which water source the two aquifers will respond to, we can estimate that groundwater flow through Qefy will increase roughly 15-20% due to the proposed action.

Some of the 15-20% increase should be accomplished by thickening unconfined aquifer W1. According to the well log of PZ-6A (Ch. 6), the permeable part of aquifer W1 extends from -32 ft (bottom) to -17 ft (top), a thickness of 15 ft. Thickening the permeable part by 15% would require a rise of the water table of 2.25 ft. which is the smallest rise of several scenarios. If we assume that the bottom of aquifer W1 is at -65 ft (top of Qefb), then the aquifer thickness is 48 ft, and a +15% thickening would require a rise of the water table of 7.2 ft. This is the maximum rise in W1 of several scenarios, because it accommodates the entire groundwater flow increase in the unconfined aquifer, rather than apportioning some part of it to the confined (W1) aquifer.

However, it is difficult to know how much of the increase to apportion to the confined aquifer (W2), which is already under considerable artesian pressure. Because the pressure heads are above the ground surface at PZ-6A, the source of the water infiltrating into W2 is not likely to be the stream itself, but rather some deeper source in bedrock that has a recharge zone far upslope of PZ-6. We have no way of identifying where that recharge zone is, in order to assess its Infiltration Ratio. If we could do this, we could apportion some of the +15% groundwater flow to a steepened piezometric surface in W2, and decrease the thickening required in W1. For example, assigning 1/4 of the increase to W2 would require steepening the piezometric surface by 3.75%, and then thickening W1 by the remaining ¾ (11.25% thickening). In such a scenario, the piezometric surface of W2 would have to be steepened from its current 0.241 (290'/1205') to 0.25 (301'/1205'), requiring the surface to be 11 ft higher than present at its uphill end. This would result in an artesian head of +14 ft above the ground compared to the present +3 ft artesian head. We consider that such high artesian heads are unlikely, because: (1) the confined water would likely break out to the surface somewhere else, under such high pressures, and (2) with such a high back-pressure, it becomes progressively harder to "stuff water" into the confined aquifer at its recharge zone.

Therefore, the post-development hydrologic condition is portrayed by a +7 ft rise of the unconfined water table in W1 (or, to -10 ft BGS), and the heads in W2 are left at their current artesian level (+3 ft above ground surface).

RESULT: The minimum post-development Factor of Safety is 1.07.

8.3.6 East Cross-Section (the East Slide)

The East cross-section extends down the axis of the East Slide, beginning at its headscarp (elevation 10,030 ft) and continuing SE for a distance of 2800 ft, to the toe at an elevation of 9510 ft (Fig. 8-20). The ground surface drops 520 ft vertically over a horizontal distance of 2600 ft, indicating an average slope of 0.2 (11.3°). The upper 45% of the slide is on US Forest Service land, and the lower 55% is on private land owned by CBMR. The Pinedale glacial trimline is projected to cross the East Slide between about 9820-9850 ft elevation, but the original moraine landform is subdued, probably by slope movement.

The geology and hydrology of the East Section is interpreted from four borehole piezometers (from bottom to top, SG-5, PZ-16, SG-4, SG-3), two inclinometers (I-SG5, I-16), and P-wave and S-wave seismic tomograms. The SG-x boreholes were drilled by Resource Consultants & Engineers in 1994, whereas PZ-16 and the two inclinometers were installed as part of this study in July 2007. After drilling through clayey landslide deposits, Mancos Shale was encountered at -63 ft in SG-3 at the head of the slide; at -70 ft (“weathered shale” 15 ft thick atop competent shale) at upper center in SG-4; at -38 ft in center at PZ-16; at -70 ft (“weathered shale”) at the toe in SG-5; and at -76 ft (“weathered shale” 9 ft thick atop competent shale) in I-SG5 at the toe.

However, in the toe boreholes there was a clear shear zone above the top of bedrock within the landslide deposit sequence. The shear zone was at depths of 59-60 ft (I-SG5) and 56-57 ft (SG-5), the latter marked by “black organics and charred wood”. Each shear zone lay atop a bouldery deposit rich in Tertiary porphyry, which we interpret as glacial till. Thus, our interpretation is that the shear zones represent the basal failure plane of the landslide toe as it advanced over a landscape of till that carried a soil containing burned organics. This interpretation is supported by the trench wall exposures in the Lower trench (described in Chapter 2). There, a 30-40 cm-thick shear zone dipped into the slope (northward), juxtaposing two different landslide units, and containing abundant pieces of burned wood up to 2” in diameter. This shear zone did not directly overlay till, so it was evidently not the basal shear zone, but a higher shear zone in the toe thrust complex.

In the mid-landslide and upper-landslide areas, boreholes did not yield an unambiguous location for the basal shear zone. In SG-4, the drive sample at -101 ft was described as “white siltstone or chemicals, with some shale below, possible formational material”, and this is the only non-gray color observed in the shale portion of the log. If the white color indicated a shear zone, that shear zone lies 31 ft below the top of the “weathered shale”, and 16 ft below what we interpret as competent Mancos Shale. It is thus possible that, in the mid- and

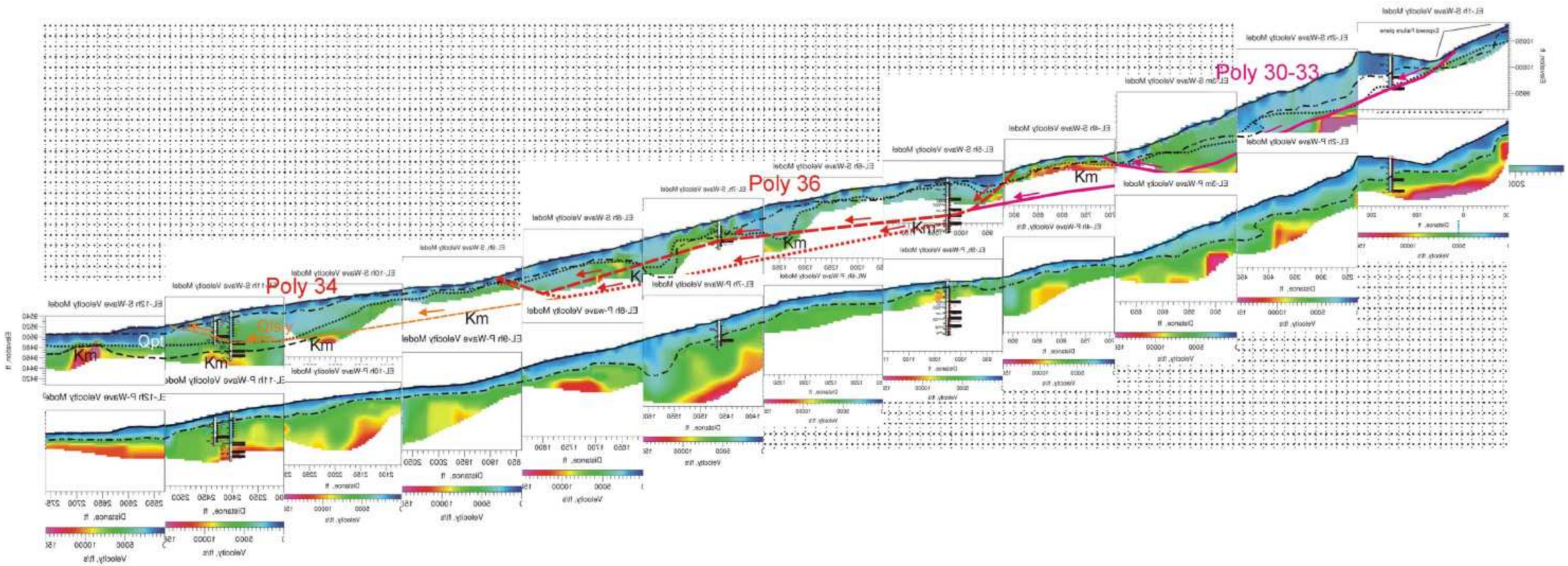

Fig. 8-20. Geologic cross-section of the East Line; NW is to the right. This section was mirrored from the original to put the uphill end at right, to match the stability modeling software. In upper section, background is the S-wave tomogram; velocities are in ft/sec. Geologic contacts are traced between boreholes (from left to right) SG-5, I-5, PZ-16, SG-4, and SG-3 along lines of constant S-wave velocity. In lower section, the background is the P-wave tomogram, from which the water table was interpreted.

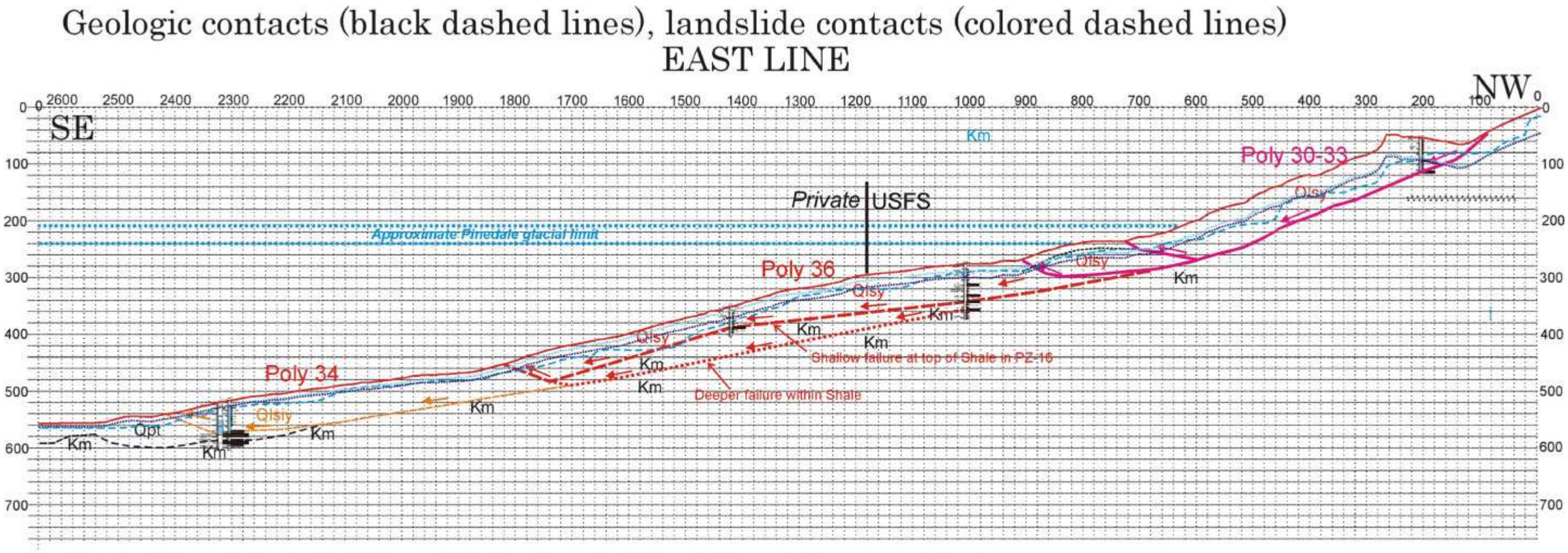

Fig. 8-21. Interpreted geologic cross-section of the East Line, without tomogram background. The water table shown is the pre-development water table. This is the section that was used in the stability analysis.

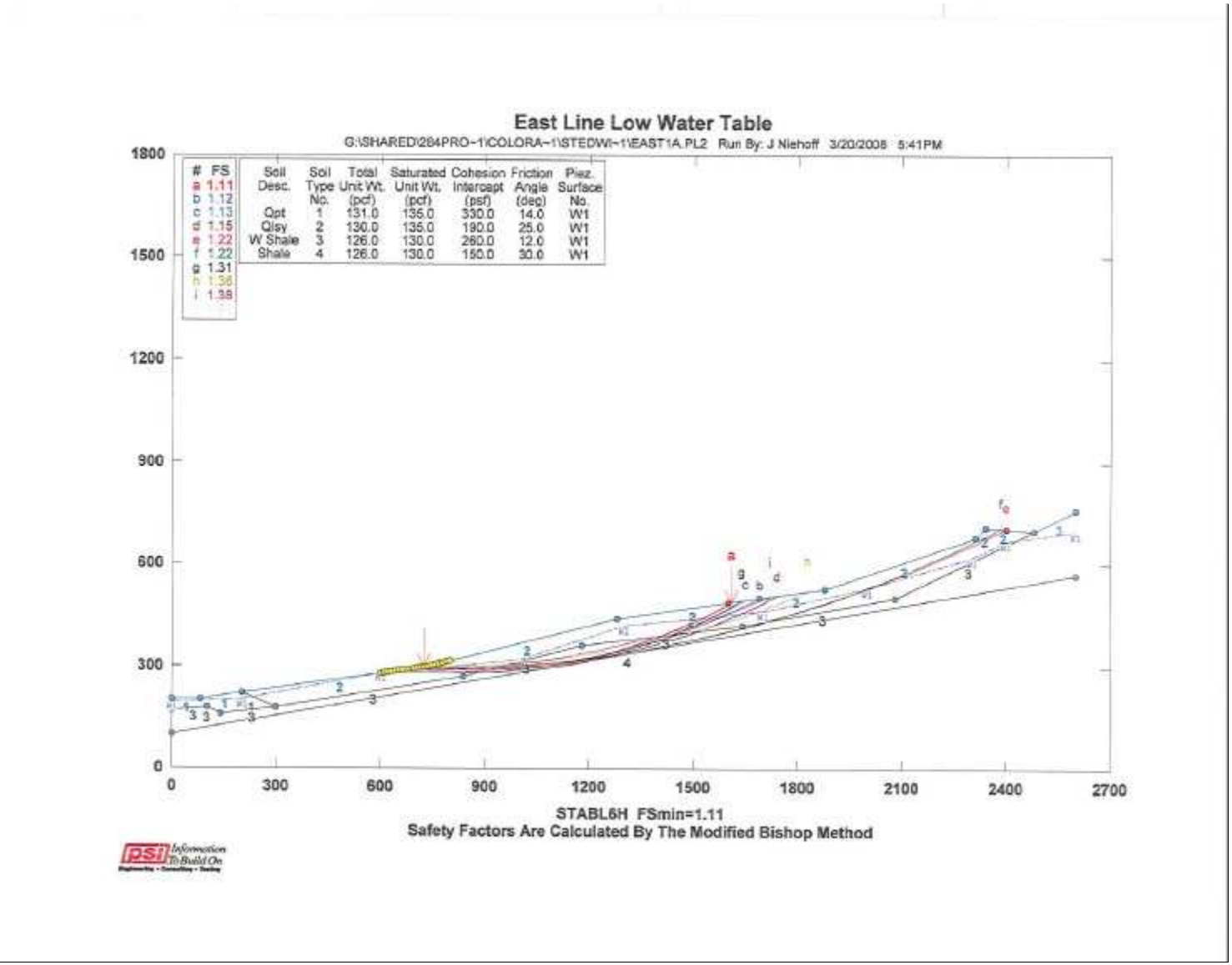

Fig. 8-22. Stability analysis of polygons 30-36 on the East Section, for pre-development conditions.

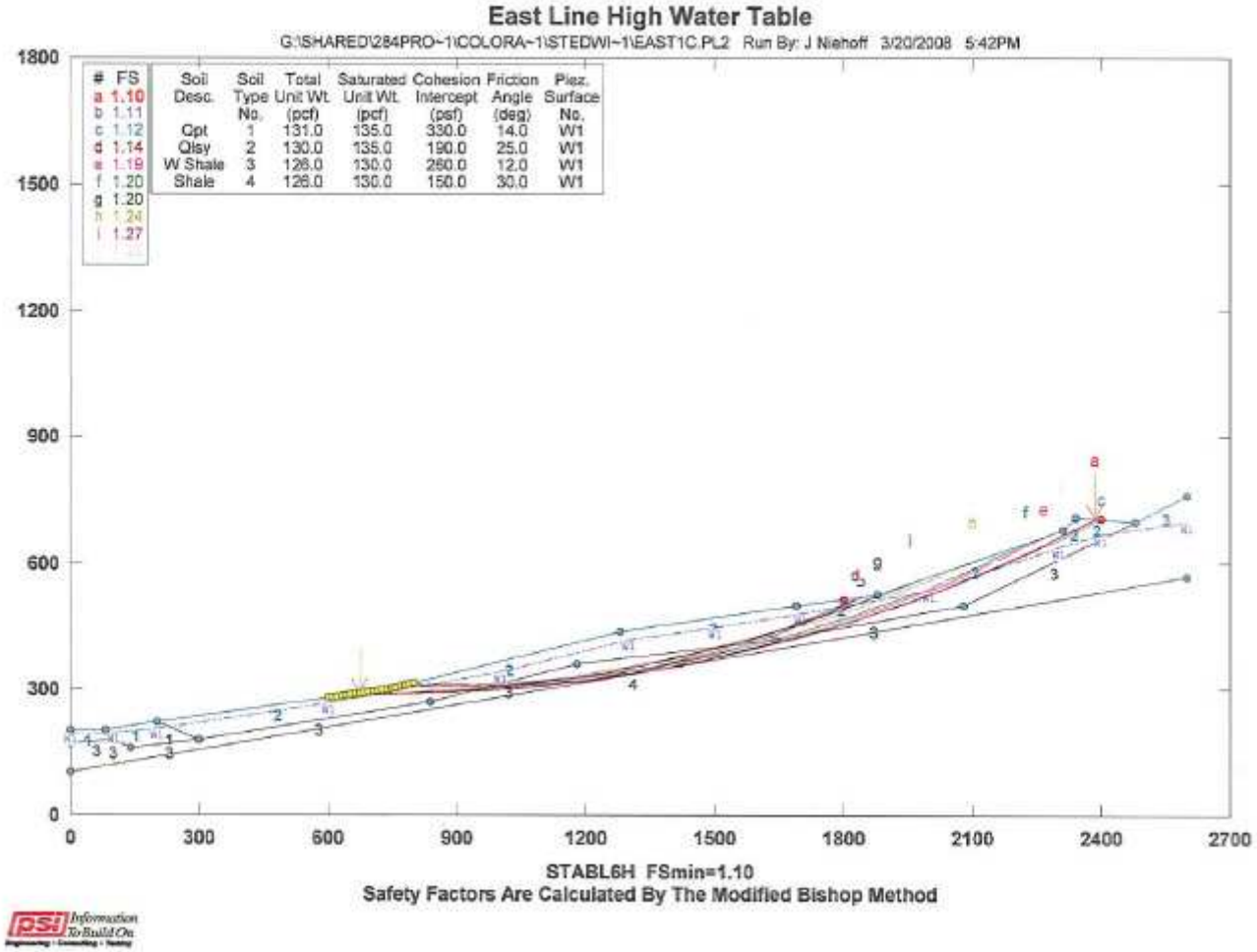

Fig. 8-23. Stability analysis of polygons 30-36 on the East Section, for post-development conditions.

upper-landslide areas, the failure plane is 15-30 ft below the top of “weathered shale”, rather than at the landslide deposit-Mancos Shale contact. Supporting evidence for such a geometry is given by the anomalously shallow depth to Mancos Shale interpreted in PZ-16, at a depth of only 38 ft. If the basal failure plane of polygon 36 were coincident with the top of Mancos Shale, it would have to rise 50 ft in the center of polygon 36 compared to its depth upslope and downslope, yet the surface topography shows no indication of bulging or internal toe thrusting at PZ-16, as would seem to be required by such a failure surface geometry. Therefore, the implication is that, at PZ-16 in the center of polygon 36, the failure plane lies within the Mancos Shale as much as 50 ft below its top.

This pattern of the basal failure plane lying within bedrock at the slide head and middle, but climbing up into the landslide deposit at the toe, was also observed by Chen and Associates (1981, 1985) in a landslide on Mancos Shale at the Buttermilk Ski Area in Aspen, CO, which reactivated in 1984 (wettest year of record). The failure plane in that study was pinpointed by bent inclinometers.

8.3.6.1 Pre-Development Stability

The geologic contacts on the section (Figs. 8-20, 8-21) were interpreted from the well logs of four piezometers and one inclinometer (from S to N, SG-5, I-SG5, PZ-16, SG-4, and SG-3) and from the S-wave tomogram (Fig. 8-20). We made no attempt to rigorously subdivide textural units within the landslide deposits atop Mancos Shale, except for the previously-mentioned shear zones. The groundwater table was deduced from the piezometers, along with the 5000 ft/sec contour on the P-wave tomogram.

Based on the boreholes and the tomograms, the East Slide appears to be a complex, 50- to -100 ft-thick, slump- translational slide sliding on a relatively planar failure surface (bedding plane?) that dips 10-11° SE. The head of the failure has to be curved, to explain the large slump block slivers of polygons 30-33. On Fig. 8-21 we show two possible failure planes within polygon 36, with a shallower one conforming to the top of Mancos Shale encountered in the boreholes, and a deeper one maintaining a more constant slope at a depth of about 80-90 ft within the Mancos Shale.

Our Upper Trench (Chapter 2) shows that the central part of the East Slide (polygon 36) has overridden the lower part (polygon 34). The nature of the contact between polygon 36 and polygons 30-33 at the head is less clear. Fig. 8-20 shows our initial interpretation, that polygon 36 is pulling away from polygons 30-33, thus the head of polygon 36 is a normal fault. This interpretation was based on our initial photo-interpretation that polygon 36 was the youngest part of the landslide. However, an alternative interpretation is that the contact is a thrust fault, and the toe of polygons 30-33 is trying to push into and override polygon 36. In this scenario, polygons 30-33 are the youngest part of the landslide, and are intimately related to the stability of polygon 36. If polygon 36 slides on its own (due to very high seasonal groundwater levels), it will de-buttress polygons 30-33. Conversely, if polygons 30-33 begin to slide (due to their steep overall slope)

and their toe presses on the head of polygon 36, that would induce a large lateral load that might destabilize polygon 36.

Unlike some of the other landslides, the East Slide appears to contain only a single, unconfined aquifer. PZ-16 and I-SG5 were drilled for this investigation, and in both wells static water remained relatively constant immediately after drilling (i.e., it did not rise), so they are interpreted as unconfined aquifers.

In the stability analysis, we defined three unconfined piezometric surfaces. Surfaces 1 and 2 approximately parallel the ground surface at various depths. Surface 1 (dark blue dotted line on Fig. 8-21) is the static water level existing in the first week of October 2007; this is the lowest seasonal water level, according to piezometer records (Table 8-8; also see Chapter 6). The curve was constructed by copying the line of the ground surface profile, breaking the line into 3 segments defined by the 4 piezometers, and then lowering the line segments to the observed water level in each piezometer in October. Surface 2 (light blue dotted line, Fig. 8-21) is the seasonal high water table (April 20-May 1, 2007), constructed in the same manner. Surface 3 (medium blue dashed line) was drawn by following the 5000 ft/sec P-wave velocity contour in the first week of October, 2007.

Table 8-8. Depths to groundwater at various times in the East Slide.

UNCONFINED WATER	Depth to Static Water in Various Piezometers (ft)			
Date Observed	SG-5	PZ-16	SG-4	SG-3
Oct. 2007 (lowest seasonal level)	-11	-19	-23	-46.5
Apr.-May 2007 (highest seasonal level)	-9.5	-5.5*	-13.5	-40

* may be weakly confined; level upon drilling was -27 ft in Nov. 2006, but by Jan. 2007 had risen to -18.5 ft

RESULTS: The East Slide has a Factor of Safety of 1.11 under Pre-development conditions, based on a shallow, curved failure arc underlying the upper 2/3 of the East Slide.

8.3.6.2 Post-Development Stability

The East Slide is defined as a “Zone of No Disturbance” in the 21-JUN-2007 design for Snodgrass Ski Area. However, the weighted Infiltration Ratio for the East Section is greater than 1.00, because of our method of averaging Infiltration Ratios of the entire subwatersheds transected by the cross-section line. Two of the four sub-watersheds crossed by the line will experience development actions, although not on the East Slide.

To remain consistent with the other cross-sections, we compute the weighted Infiltration Ratio based on whole sub-watersheds, which yields a value of 1.05, associated with a post-development rise in the water table of 1.3-1.7 ft (average 1.5 ft). This rise can also account for some development actions adding water to slopes far upslope of the East Slide (for example, in the Chicken Bone

area), which could conceivably enter the East Slide via long subsurface flow paths.

RESULTS: The East Slide has a Factor of Safety of 1.10 under Post-development conditions. This value is only a slight decrease from the pre-development conditions, due to the minimal impact of development on the slide.

8.4 Potential of New Shallow Landslides (infinite-slope failures such as the Gold Link Slide of 2000)

8.4.1 Background

The Gold Link landslide of 2001 on Mt. Crested Butte represents a type of shallow landslide that might also occur on Snodgrass Mountain, but which has not been previously analyzed in this report. Although the Gold Link slide may have occurred on ancient landslide deposits, it did not represent a full-thickness reactivation of a thick (40-80 ft) landslide, as was analyzed in the previous section. Instead, the Gold Link slide was a shallow (5-8 ft thick) debris slide-debris flow failure that occurred in a ski trail. This failure type involves detachment of a thin, often saturated, “slab” of earth material from a slope, that breaks up and partially liquefies after it has moved a few tens of feet. The liquefied material turns into a runny debris flow that continues downslope for hundreds of feet, before coming to rest on gentler slopes at the base of the hill. Because the geology of the Gold Link failure site is virtually identical to the geology of the SE slope of Snodgrass Mountain, similar failures may occur in ski trails constructed on Snodgrass, if conditions are similar.

As explained in Chapter 1, the hazard posed by various landslide types depends on movement velocity. Debris flows are the fastest movement type that might occur on Snodgrass, and the only slide type that poses a, immediate hazard to human health and safety. Therefore, in this section we analyze the probability of future debris slide-debris flow failures occurring on Snodgrass due to trail clearing and snowmaking.

The failed ski trail at Gold Link had a gradient of 17°. Following the analogy described above, ski trails constructed at Snodgrass on ancient landslide terrain sloping at or above 17° may also be susceptible to failure. Fortunately, most of the landslide complex on the SE flank of Snodgrass Mountain is composed of slopes gentler than 17° (Fig. 8-24). Slopes steeper than 17° are restricted to five general areas. One of those areas (the “small slope band”) contains no proposed development actions. The other four areas do contain proposed trails

Table 8-9. Characteristics of slope areas steeper than 17° on Snodgrass where trails and snowmaking are proposed.

Area	Proposed trails	Proposed snowmaking	Potential detachment zone; hazards and infrastructure at risk	Potential runout zone; hazards and infrastructure at risk
East Facet	11, 12, 13, 14	On 12 and 13	Hummocky triangular face of the East Facet; heavily forested; underlain by coarse-grained, well-drained residual soils developed on Tertiary porphyry; very few small slumps **Contains East Lift** ,which ascends entire facet, along S edge of trail 14 **Main Lift** ascends extreme west edge	Chicken Bone meadow, 67 acres; **contains Snodgrass Road**
West Facet	1, 2, 3, 3A	On 2	Hummocky triangular face of the East Facet; heavily forested; underlain by both shale- and porphyry-derived soils; many landslides mapped **No infrastructure**	West Slide Complex, 48 acres; **no infrastructure**
Steep slope band	11, 12	On 11, 12	Main Lift crosses slope band	Old earthflow (11 acres) and summit of Slump Block; contains top terminal of Gold Link/North Village lift; bottom terminal of Main Lift
East slope band	C3a, C3b, C2c	C2a, C2c	Snodgrass Road traverses steep slope, in the vicinity of the switchback	East Lift diagonals across N end of slope band

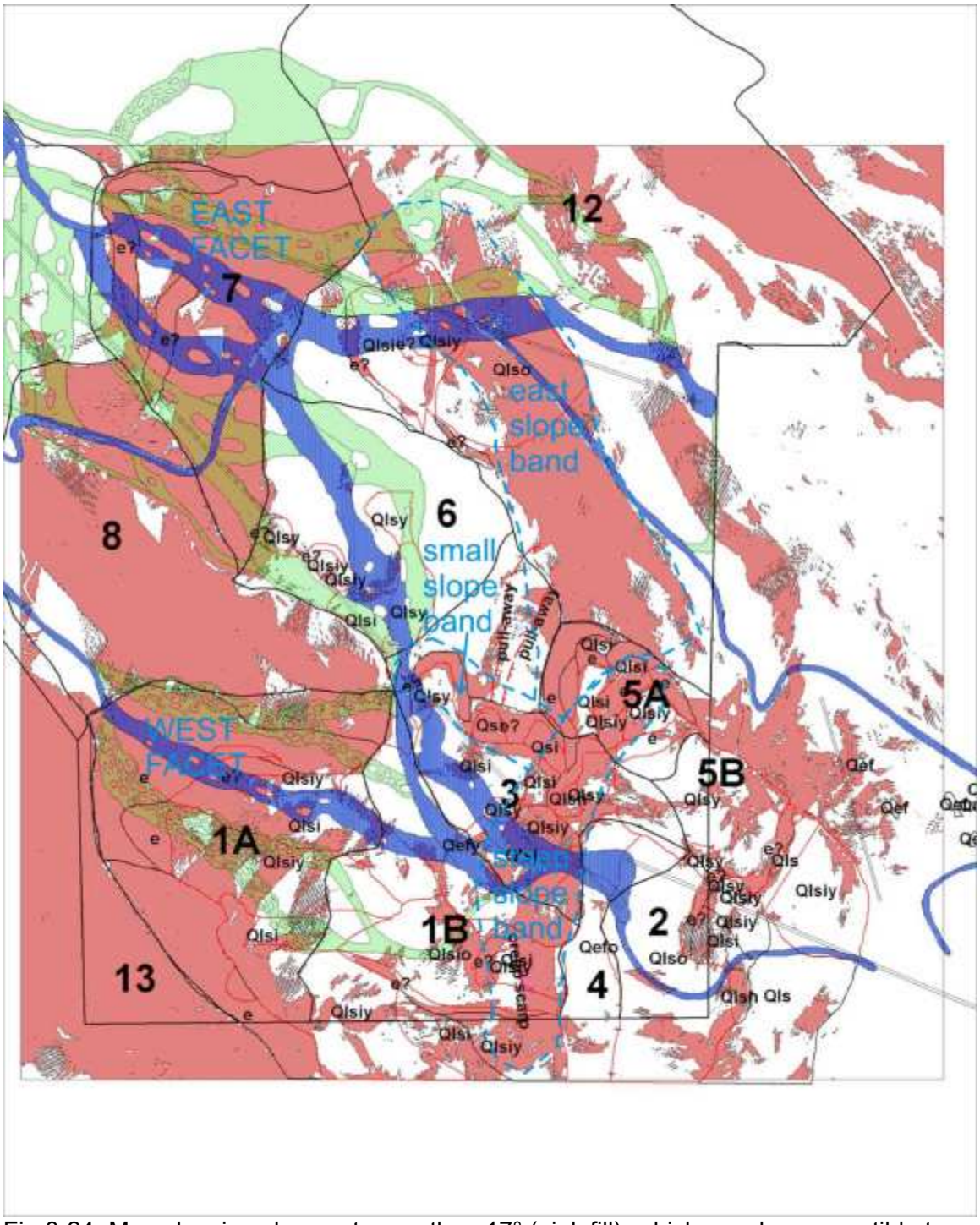

Fig.8-24. Map showing slopes steeper than 17° (pink fill), which may be susceptible to shallow debris slide-debris flow failures. Black rectangular outline is Snodgrass permit boundary, large numbers are GHUs. Landslide polygons are outlined in red, trails have green fill, snowmaking has blue fill. Thin double lines represent proposed lifts. Slopes steeper than 17° are concentrated on the East and West Facets, and on three distinct slope bands (steep slope band, small slope band, east slope band), outlined by blue dashed lines.

8.4.2 Results

Although we have some geotechnical measurements and water table information for deep landslides (described previously), we have no direct data on these parameters for the shallow slope-mantling deposits on steep slopes across the project area. Thus, predicting the probability of slab failures across the entire development area would require so much detailed data, it is beyond the scope of this study.

Instead, we can assume there is a small probability of debris slide- debris flow failures in the steep slope bands, and concentrate our efforts on protecting whatever infrastructure exists in the detachment zone and in the runout zone, from Gold Link-type events. The most critical buildings in the runout zone of any steep slope zone are the 2 lift terminals below the steep slope band. In Fig. 8-24, we show a proposed debris deflection berm that would divert any possible flow material emanating from the steep slope band. Compared to these lift terminals, all the other infrastructure at risk is relatively minor (individual lift towers, access road). Lift towers experience little damage from deposition of debris flow material, due to the immobility of the tower base. Roads can be protected from debris flow by judicious culverting, but this is a standard engineering practice.

Overall, it does not seem that the probability of debris slide-debris flow failures is particularly high on Snodgrass Mountain (for example, we mapped no identifiable debris flows during the landslide inventory mapping), nor is much critical infrastructure at risk to those processes.

8.5 Variations in Future Factors of Safety with Time

The three maxima of the snowpack data on Mt. Crested Butte fall 11 years apart (1984 to 1995) and 12 years apart (1995 to 2007). Although this may be a coincidence, it may also represent an effect of the 11-year cycle in solar radiance (http://www.agu.org/revgeophys/reid00/node3.html). The only times that the cumulative hydrologic effects of the Snodgrass proposed action are likely to exceed the hydrologic effects that the mountain has already experienced from natural snowpack, is once every 11-12 years. The reason can be seen on Fig. 8-x.

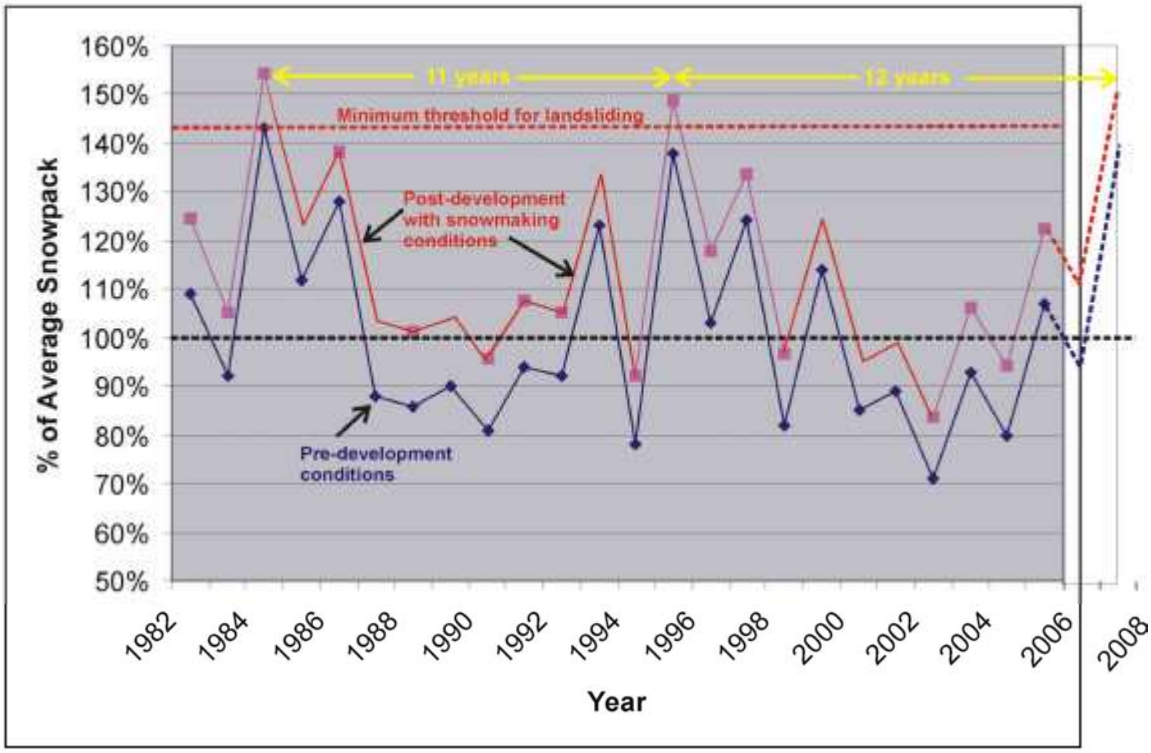

Fig. 8-24. Conceptual diagram showing how the predicted hydrologic effects of the proposed action on Snodgrass (red line) will add to natural fluctuations in snowpack (precipitation) from year to year (blue line). The red & purple line was created by adding the post-development increase in runoff at stream Node A3 (bottom of Snodgrass), which is a surrogate for other hydrologic increases such as groundwater rise. The horizontal red dashed line shows the extreme hydrologic condition of the past 24 years, which fell short of triggering observed landsliding on Snodgrass (minim estimate of threshold for slope instability). We anticipate that the 2007-08 snow year will also be an extreme year (dashed lines). Based on the historic snowpack record on Mt. Crested Butte, that minimum threshold will likely only be exceeded in extreme years, which occur every 11-12 years.

When we superimpose the additional hydrologic effects from the proposed action, onto the natural snowpack fluctuations of the past 24 years, we see that the additional effect is not large enough to exceed the minimum threshold except in the extreme years. That is because the increment of water (runoff. infiltration) added by the development actions on the SE flank of Snodgrass only ranges from +18% in dry years, to +14.5% in average years, to +7.8% in wet years. When these values are superimposed on the natural fluctuations of snowpack over the past 24 years, the only years that exceed the minimum threshold (143% of normal) are the extreme years that occur once every 11-12 years (Fig. 8-x).

Obviously, if the predicted hydrologic effects of the proposed action were larger (say, +20% in wet years, rather than the modeled +7.8%), then some of the larger *non-extreme* snowpack years might also exceed the 143% threshold (such as 1996, where 128% + 20%= 148%). But the modeling performed by RESOURCE (Chapter 5) shows that the hydrologic additions of the proposed action become proportionally smaller in wet years, due to being “swamped” by the huge volume of the natural snowpack.

In addition, this minimum threshold for slope instability is still smaller than the level at which landslides move on Snodgrass. How much smaller, we do not know. We do know that the level was reached in 1984 and nearly reached again in 1995, yet in neither years was landslide movement observed on Snodgrass. Thus, the conceptual analysis suggests that it will take larger snowpacks (or faster snowmelt) than have occurred in the past 24 years, to reactivate the Snodgrass landslides. The probability of that reactivation happening reaches a peak every 11-12 years, but in the past 24 years the water levels have not reached the true threshold level for landslide reactivation. The conceptual analysis indicates that this same situation is likely to continue even after the proposed development.